表4. 算出された補正係数値

No.	N法	B法	S法	M法
1	1.00	0.44	0.35	0.62
2	1.00	0.48	0.27	0.62
3	1.00	0.46	0.38	0.51
4	1.00	0.44	0.48	0.59
5	1.00	0.43	0.34	0.45
6	1.00	0.31	0.29	0.34
7	1.00	0.52	0.43	0.46
8	1.00	0.64	0.67	0.57
9	1.00	0.63	0.55	0.56
10	1.00	0.54	0.62	0.58
Mean (f)	*1.00*	*0.49*	*0.44*	*0.53*

(N法測定値/各法測定値)

表5. 補正後の4法のインヒビター結果

No.	N法	B法	S法	M法	CV%
1	1.47	1.62	1.82	1.27	15.3
2	1.85	1.90	2.99	1.57	30.0
3	2.07	2.18	2.36	2.16	5.6
4	3.32	3.70	3.07	2.96	10.0
5	3.38	3.86	4.38	4.02	10.6
6	3.54	5.53	5.41	5.54	19.6
7	5.61	5.23	5.68	6.40	8.5
8	6.02	4.62	3.92	5.61	18.9
9	6.50	5.06	5.20	6.15	12.3
10	113.58	103.38	80.05	103.95	14.2

各法の結果はBU/ml

から同一の測定法による結果と誤解されることも少なくない．また，インヒビター測定には様々な変動要因が指摘されており[5]，中でもFVIII：Cの測定に使用するAPTT試薬の組成(リン脂質，活性化剤)とインヒビター間で認められる反応性の違いは著しく[6]，異なるインヒビター測定法の混在に加え，さらなる問題点も抱えている．われわれは，これまでにFVIIIインヒビター陰性の血友病A患者検体を対象としてインヒビター測定法4法について検討し，その特性に差異があることを報告した[4]．今回さらに，インヒビター陽性の血友病A患者検体を対象として，同様にインヒビター測定法4法について比較検討した．

はじめに4法の検体希釈法について，FVIII欠乏血漿を被検材料に用いpHとFVIII：Cの変化を比較検討した．N法では検体希釈に伴う差異は観察されなかったが，被検血漿と希釈液の両者がともにFVIII欠乏血漿で，同じ反応液条件となるためと思われた．これに対し，緩衝液で希釈するB法，M法では検体希釈に伴った中性域へのpH変化が観察され，反応液中の緩衝液比率の漸増によってもたらされる変化と考えられた．また，このときFVIII：Cは1倍でB法；29.1%，M法；18.8%であったが，希釈液のみの反応液ではそれぞれ46.5%，39.6%と両測定法内で大きな差を認め，このことは，既にわれわれが報告したインヒビター測定時における反応液pHとFVIII：C測定値の負の関係[4]と同様の結果(すなわち，反応液のpHが中性域へと低下するにつれて，FVIII：C測定値は上昇する)と考えられた．実際のインヒビター測定時において，B法では緩衝液のみの反応液が対照反応液であるため，今回検討した1倍反応液がそのままFVIII残存活性62.6%となり，ゆえにインヒビター値は0.68BU/mlと求められて「陽性」と判定される値となってしまう．一方，M法では，同じ血漿成分比率に保持された条件下の測定反応液と対照反応液から残存活性を求めるため，希釈に伴うpH等の液性差は小さく，偽陽性を示すことは少ないと考えられる．また，生理食塩水で希釈するS法は，pH 8.3前後と高いものの変動は小さくFVIII：C変化も軽度であったが，pH緩衝作用の無い生理食塩水がもたらす結果と考えられた．

インヒビター陽性血友病A患者血漿10検体を対象とした4法の各インヒビター値の比較成績(表3)をみると，方法の違いによるインヒビター値のバラつき程度は著しく，低い検体希釈倍率でより大きいCV値が観察された．また，平均値に対する比で各法を比較した結果では，ISTH/SSCの推奨法であるN法と比較して他の3法のインヒビター値は有意に高く($p<0.001$)，とりわけS法が高値を示すことが明らかとなった．この成績は，N法で5BU/ml未満であった6

例のうち，S法で5例，B法およびM法で3例が5BU/ml以上を示したこととも符合することから，これら4法間の較差を明確に反映した成績と解釈された．

N法を基準として方法ごとに算出した補正係数を適用した補正後の比較成績では，著明な高値例のNo.10を含め前述した方法間のバラつきが補正後にCV値5.6%～30.0%と顕著に改善し，各法間の有意差も認めず，さらに，5BU/mlを基準とした4法間の判定も，補正前の一致率5/10（50%）に比べて補正後は8/10（80%）と向上した．この成績は，補正係数の適用によって各法の測定較差が適切に是正され，さらに，N法以外の方法で得たインヒビター値であってもよりN法に準じた値として評価し得ることを示唆している．これまでにも，new Oxford法とB法間では平均1.21倍の較差があることが示されており[7]，今回の補正係数もこれと同様に各方法間の較差を表していると思われる．

これまで，各種インヒビター測定法についてその測定特性や差違を詳細にした報告は少なく，また，検査企業に委託される場合が多い今日においては，報告された値から測定方法の違いを察知し比較することは困難であると考えられる．今回示された各インヒビター測定法間の差違を理解し把握することは血友病A患者の止血管理において重要と思われ，加えて，ISTHが推奨するN法がその煩雑さ故に日常検査法として普及しにくい点を考慮すると，補正係数を用いた結果値の評価は，現時点において日常検査法として簡便に利用できる方法であり，従来の測定値をより有用な治療選択の指標として活用し得る方法であると思われた．しかしながら，使用するAPTT試薬の特性も較差の要因となり得ることから，使用する測定法とN法との較差を確認した上で結果の解釈を行う事が望ましいと考えられた．

結　論

FVIIIインヒビター陽性検体を対象として，4つのインヒビター測定法を比較検討した．

1）各法より得られるインヒビター値には明らかな差異を認め，反応液の違いや希釈操作の違いが要因となることが示唆された．とくに，Bethesda法の希釈操作は大きな変動要因となると考えられた．

2）Nijmegen法に比較して，Bethesda法，Bethesda変法（S法，M法）は有意に高いインヒビター値を示した（$p<0.001$）．

3）Nijmegen法を基準とした補正法の適用により，従来の各法のインヒビター値を容易に比較し得る可能性が示唆され，日常の血友病Aの止血管理において有用と考えられた．

文　献

1）瀧　正志：血友病患者のインヒビター．血栓・止血・血管学—血栓症制圧のために—　一瀬白帝編，p402—409，中外医学社，東京，2005.

2）Verbruggen B, et al: The Nijmegen modification of the Bethesda assay for factor VIII: C inhibitors: improved specificity and reliability. Thromb and Haemost 73: 247—251, 1995.

3）Kasper CK, et al: A more uniform measurement of factor VIII inhibitor. Thromb Diathes Haemorrh 34: 869—972, 1975.

4）山崎　哲，他：第VIII因子インヒビター測定の特性および不活化処理の有用性．日本血栓止血学会誌　19（2）：235—243，2008.

5）2006 Minutes and Annual Reports; ISTH/SSC, Factor VIII inhibitor assays, (http://www.med.inc.edu/isth/ssc/06sscminutes/06factorviiifactorix.html)

6）山崎　哲，他：循環抗凝血素を有する症例における凝固因子活性測定．日本検査血液学会雑誌　7（2）：270—277，2006.

7）Austen DEG, et al: A comparison of the Bethesda and new Oxford methods of factor VIII antibody assay. Thromb Haemost 47: 72—75, 1982.

Abstract

Methodological characteristics of Factor VIII: C inhibitor assays, and an evaluation by the application of correction factor

Satoshi Yamazaki[1)], Noriko Yamazaki[1)], Noriko Suzuki[1)], Hiromi Goto[1)], Shigenobu Takayama[2)], Masashi Taki[3)]

[1)]Department of Clinical Laboratory, St. Marianna University School of Medicine Hospital, 2-16-1, Sugao, Miyamae-ku, Kawasaki, Kanagawa, 216-8511 Japan

[2)]Faculty of Health Science, Daito Bunka University

[3)]Department of Pediatrics, St. Marianna University Yokohama City Seibu Hospital

In recent years, for the FVIII inhibitor assay, the Nijmegen method has been recommended by the ISTH. However, it has not yet become common in Japan, and the Bethesda method is still widely used, and modified Bethesda methods also exist.

To clarify the differences between these methods, we compared four FVIII inhibitor assays: the Nijmegen (N), Bethesda (B), and two (S and M) modified Bethesda methods. The two modified methods use pre-treated plasma with an inactivation treatment of coagulation factors at 56℃, method S uses FVIII deficient plasma, and method M uses normal plasma as a control.

In a comparison of sample dilution procedures using FVIII deficient plasma, the N and S methods, with nearly the same pH values in all of the tested samples, showed a constant FVIII: C. However, methods B and M, with a decrease in pH due to sample dilution, showed an elevated FVIII: C of 12%～16%, according to their pH changes.

The results for 10 samples with FVIII: C inhibitor varied remarkably (CV: 22%～55%; mean, 34.6%) among the four methods. The inhibitor values from B, S, and M were significantly higher than the values from method N ($p < 0.001$). Especially, the six cases of <5BU/ml validated by method N were indicated as >5BU/ml in five cases by method S, and in three cases by methods B and M.

By application of the correction factors obtained based on method N, the CV variations were improved markedly to 5.7%～30.0% (mean, 14.5%). Furthermore, the discrepant six cases were corrected, decreasing to two cases in S and B, and to one case in method M.

These results have clearly shown that the inhibitor values obtained via the four methods differ, which may be due to differences in the dilution procedures. An application of the correction factor based on method N may be useful for comparing the inhibitor values.

Key words: Factor VIII, Inhibitor, Haemophilia A, Bethesda method, Nijmegen method

Biochemical and Biophysical Research Communications 400 (2010) 323–328

Contents lists available at ScienceDirect

Biochemical and Biophysical Research Communications

journal homepage: www.elsevier.com/locate/ybbrc

Vinculin activates inside-out signaling of integrin αIIbβ3 in Chinese hamster ovary cells

Tsukasa Ohmori [a,*], Yuji Kashiwakura [a], Akira Ishiwata [a], Seiji Madoiwa [a], Jun Mimuro [a], Shigenori Honda [b], Toshiyuki Miyata [b], Yoichi Sakata [a,**]

[a] Research Division of Cell and Molecular Medicine, Center for Molecular Medicine, Jichi Medical University, Tochigi, Japan
[b] National Cardiovascular Center Research Institute, Osaka, Japan

ARTICLE INFO

Article history:
Received 11 August 2010
Available online 20 August 2010

Keywords:
Integrin
Vinculin
Signal transduction
RNA interference
Platelets
Talin
Actin

ABSTRACT

Although vinculin is used frequently as a marker for integrin-mediated focal adhesion complexes, how it regulates the activation of integrin is mostly unknown. In this study, we examined whether vinculin would activate integrin in Chinese hamster ovary (CHO) cells expressing human integrin αIIbβ3. Silencing of vinculin by lentiviral transduction with a short hairpin RNA sequence affected the binding of PAC-1 (an antibody recognizing activated human αIIbβ3) to a constitutively active form of αIIbβ3 (α6Bβ3) expressed on CHO cells, while its inhibitory effects were much weaker than those of talin-1. Overexpression of an active form of vinculin without intramolecular interactions, but not the full length one, induced PAC-1 binding to native αIIbβ3 expressed on CHO cells in a manner dependent on talin-1. On the other hand, silencing of talin-1, but not vinculin, failed to induce cell spreading of α6Bβ3-CHO cells on fibrinogen, even in the presence of PT 25-2, a monoclonal antibody that activates αIIbβ3. Thus, an active form of vinculin could induce αIIbβ3 inside-out signaling through the actions of talin-1, while vinculin was dispensable for outside-in signaling.

1. Introduction

Vinculin is a highly conserved actin-binding protein that is frequently used as a marker for integrin-mediated focal adhesion complexes [1,2]. Although vinculin itself does not directly bind to integrins, it is thought to play key roles in focal adhesion assembly and in cell adhesion by connecting talin and α-actinin to the actin cytoskeleton [1,3]. Previous studies have suggested that vinculin contains a globular head domain, a flexible neck and a tail domain. The head and tail domain are connected by the flexible proline-rich neck region and interact to form a closed, autoinhibited conformation that masks the binding sites for many other cytoskeletal proteins [2,4]. Vinculin is also critical for proper embryonic development, because all homozygous vinculin$^{-/-}$ embryos die because of brain and heart defects [5]. Despite extensive reports on the structure of vinculin and its associations with other cytoskeletal proteins, its precise roles in directly modulating the ligand-binding capacities of integrins remain to be elucidated.

Blood platelets are terminally differentiated anucleate cells that are responsible for primary hemostasis and pathological thrombosis. Platelets express members of the integrin β1 subfamily that support platelet adhesion to extracellular matrix proteins, as well as expressing members of the integrin β3 subfamily [6]. Among them, integrin αIIbβ3, a receptor for fibrinogen, von Willebrand factor, fibronectin and vitronectin, is an essential requirement for platelet aggregation [7]. This molecule is suitable for studies of integrin receptors because it is well characterized with respect to its ligand binding and signal transduction. In this study, we employed CHO cells expressing αIIbβ3 to investigate the roles of vinculin in modulating the ligand-binding capacities of integrins. We found that the activated form of vinculin can increase the affinity of αIIbβ3 through the actions of talin-1.

2. Materials and methods

2.1. Materials

The materials used in this study were obtained from the following suppliers: PAC-1 (a monoclonal antibody (mAb) recognizing

Abbreviations: CHO, Chinese hamster ovary; mAb, monoclonal antibody; APC, allophycocyanin; aa, amino acid; EGFP, enhanced green fluorescent protein; HIV, human immunodeficiency virus; sh, short hairpin; MOI, multiplicity of infection; ILK, integrin-linked kinase; PIP2, phosphatidylinositol (4,5)-bisphosphate.

* Corresponding author. Address: Research Division of Cell and Molecular Medicine, Center for Molecular Medicine, Jichi Medical University, 3111-1 Yakushiji, Shimotsuke, Tochigi 329-0498, Japan. Fax: +81 285 44 7817.

** Corresponding author. Address: Research Division of Cell and Molecular Medicine, Center for Molecular Medicine, Jichi Medical University, 3111-1 Yakushiji, Shimotsuke, Tochigi 329-0498, Japan. Fax: +81 285 44 7817.

E-mail addresses: tohmori@jichi.ac.jp (T. Ohmori), yoisaka@jichi.ac.jp (Y. Sakata).

0006-291X/$ - see front matter © 2010 Elsevier Inc. All rights reserved.
doi:10.1016/j.bbrc.2010.08.056

activated human integrin αIIbβ3) and anti-paxillin mAb (clone 349; BD Biosciences Co., San Jose, CA); horseradish peroxidase-conjugated anti-green fluorescent protein (GFP) polyclonal antibody (Acris Antibodies GmbH, Himmelreich, Germany); allophycocyanin (APC)-conjugated anti-mouse IgM (eBioscience Inc., San Diego, CA); anti-talin mAb (clone 8D4; Sigma–Aldrich Co., St. Louis, MO); anti-vinculin mAb (clone V284; Chemicon International Inc., Billerica, MA); anti-human integrin αIIbβ3 mAb (clone 5B12; DakoCytomation, Glostrup, Denmark); PT 25-2 (a mAb that activates human integrin αIIbβ3; Takara Bio Inc., Otsu, Japan) [8].

2.2. cDNA cloning, construction of lentiviral vectors and virus production

cDNAs for mouse vinculin and talin-1 were cloned as described [9]. Truncated cDNA fragments of vinculin (amino acids (aa) 1–258, 1–880 and 881–1066) were amplified by polymerase chain reaction (PCR). A constitutively active form of vinculin (T 12) [3] was created using a Quick Change Site-directed Mutagenesis Kit (Stratagene Corp., La Jolla, CA). The primer pairs used in this study are shown in Supplementary Table 1. Enhanced green fluorescent protein (EGFP)-fusion proteins were created by insertion of various cDNAs into the sequence of pEGFP-C plasmid (Clontech Laboratories Inc., Mountain View, CA).

A gene transfer vector, pLL3.7, for constructing replication-defective self-inactivating human immunodeficiency virus (HIV) lentiviral vectors expressing short hairpin (sh) RNA sequences (LentiLox vectors) was purchased from ATCC (Manassas, VA). We selected two shRNA sequences for mouse vinculin, designated Vin-B and Vin-C and cloned them into the pLL3.7 lentiviral vector plasmid (LentiLox) [10]. The shRNA sequences for control (Random) or talin-1 (Talin-A) were as reported [9]. To create HIV lentiviral vectors for protein expression, the pLL3.7 lentiviral vector was digested with XbaI and EcoRI to delete the sequence from the U6 promoter to EGFP and each EGFP-fusion protein sequence driven by the CMV promoter derived from the pEGFP-C plasmid was then inserted. The lentiviral vectors were essentially generated as described [9–11].

2.3. Immunoblotting

Immunoblotting with specific antibodies was performed as described previously [9,10].

2.4. PAC-1 binding to αIIbβ3-CHO cells

A chimera of the αIIb extracellular and transmembrane domains joined to the α6B cytoplasmic domain was cotransfected with integrin β3 into CHO-K1 cells [12]. The chimeric integrin (α6Bβ3) is a constitutively active form that spontaneously binds to PAC-1 [13]. We also cloned CHO cells expressing the native form of human integrin αIIbβ3. The oligonucleotide primer pairs used for cDNA cloning are shown in Supplementary Table 1. CHO cells ($2–4 \times 10^4$) expressing α6Bβ3 (α6Bβ3-CHO cells) or native human

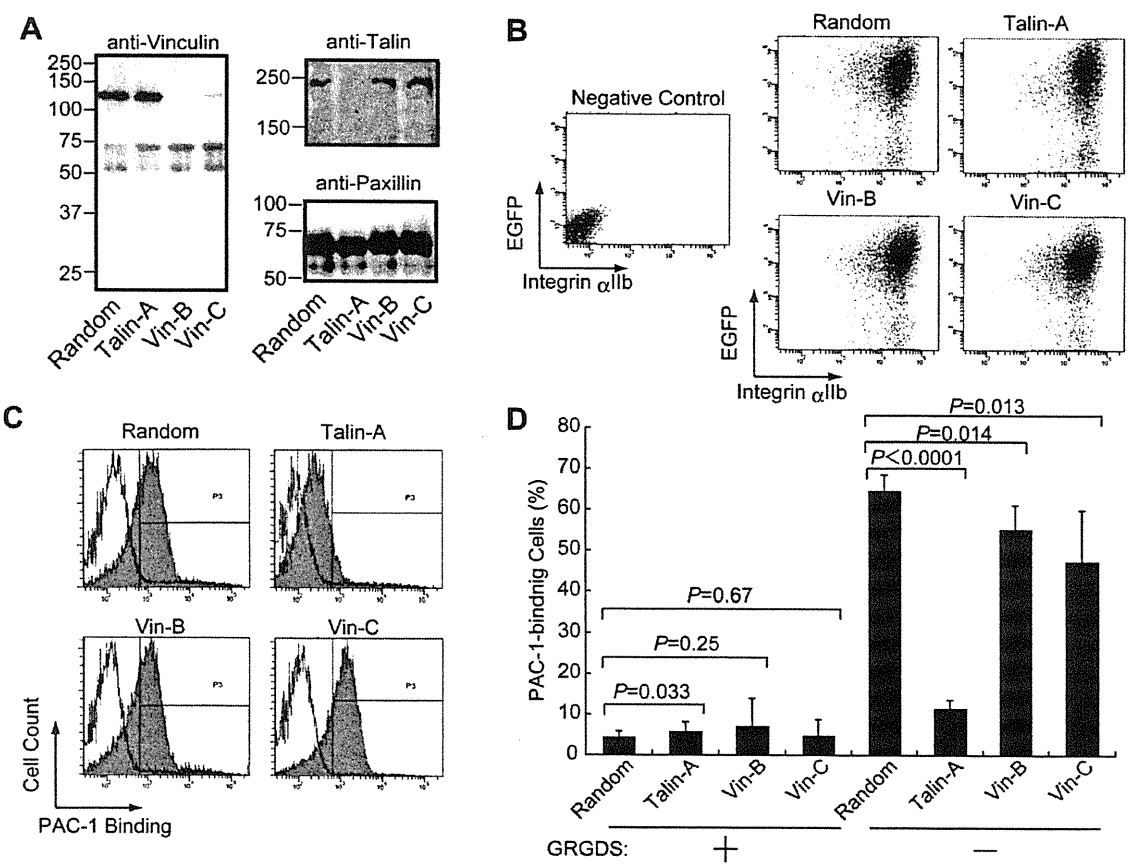

Fig. 1. Loss of vinculin marginally affects the integrin activation status in α6Bβ3-CHO cells. Cells were transduced with the indicated LentiLox vectors at a multiplicity of infection (MOI) of 3. (A) Lysates obtained from the transduced cells were immunoblotted with anti-vinculin, anti-talin and anti-paxillin monoclonal antibodies (mAbs). (B) Enhanced green fluorescent protein (EGFP) expression (vertical) and αIIbβ3 expression (horizontal) were examined by flow cytometry after transduction. (C) The affinity state of integrin α6Bβ3 was assessed by PAC-1 binding in the absence (solid gray) or presence (black line) of 1 mM GRGDS. (D) Columns and error bars represent the mean ± SD of PAC-1 binding ($n = 7$). Differences between the two groups were analyzed statistically using Student's t test.

integrin αIIbβ3 (αIIbβ3-CHO cells) were allowed to adhere to 12- or 6-well plates for 16 h and then transduced with various LentiLox vectors or HIV vector at a multiplicity of infection (MOI) of 3. The PAC-1-binding activities and protein expressions were assessed after 72–96 h. Subsequently, the cells were resuspended in Hepes/Tyrode buffer containing 1.5 mM $CaCl_2$ and incubated with or without 1 mM GRGDS. The cells were then incubated with 1 μg of PAC-1 and the antibody binding was detected with an APC-conjugated anti-mouse IgM antibody. To transduce the cells with two HIV vectors for a target EGFP-fusion protein expression vector and shRNA, the cells were simultaneously transduced with an HIV vector to overexpress the target protein at a MOI of 3 and with a LentiLox vector at a MOI of 6 (see Fig. 4A). For these experiments, we removed the DNA sequence for the EGFP gene driven by the CMV promoter from the LentiLox plasmid by digestion with NsiI and EcoRI.

2.5. Adhesion of CHO cells to fibrinogen

Cell adhesion to fibrinogen was assayed in 8-well Lab-Tek® Chamber Slides™. The chambers were coated with 500 μg/ml of fibrinogen for 16 h at 37 °C, washed twice with phosphate buffered saline (PBS) and blocked with 10 mg/ml of bovine serum albumin (BSA) for 1 h. The transduced CHO cells were placed in the fibrinogen-coated chambers for 120 min at 37 °C. After two washes with PBS, adherent cells were fixed with 3% paraformaldehyde in PBS for 40 min and then permeabilized with PBS containing 0.3% Triton X-100 and 5% donkey serum for 2 h. After washing with PBS, the cells were incubated with an anti-paxillin mAb (1:500) for 16 h at 4 °C, washed in PBS and incubated with an Alexa 488-conjugated goat anti-mouse IgG polyclonal antibody (Molecular Probes Inc., Eugene, OR) for 2 h. Actin filaments were detected simultaneously by staining with 1 μg/ml of rhodamine-conjugated phalloidin. After mounting in Vectashield® with DAPI (Vector Laboratories Inc., Burlingame, CA), the immunofluorescence staining was observed and photographed using a confocal microscope (FV1000; Olympus, Tokyo, Japan). When required, the cell area was quantified using NIH Image J Ver. 10.2 for Macintosh (NIH, Bethesda, MD; http://rsbweb.nih.gov/ij/) by a blinded observer.

3. Results

3.1. Expression of the activated form of vinculin induces inside-out signaling of integrin αIIbβ3

To examine the effects of vinculin silencing on integrin activation, we first employed CHO cells (α6Bβ3-CHO cells) expressing the chimeric integrin α6Bβ3 in a constitutively energy-dependent

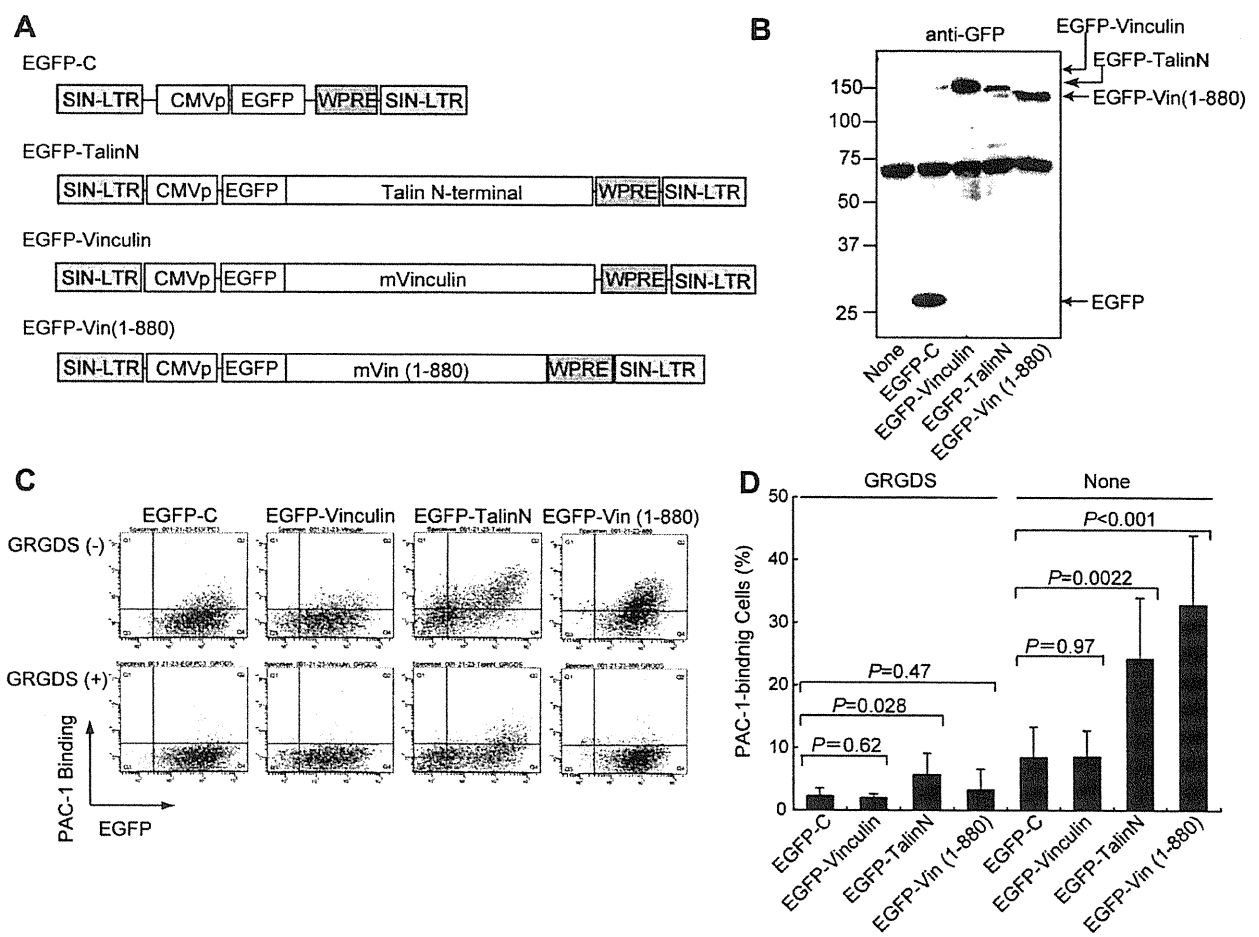

Fig. 2. Overexpression of the vinculin N-terminal domain, but not full-length vinculin, induces activation of native integrin αIIbβ3 in CHO cells. (A) Schematic representations of the HIV vector constructs used in this experiment. (B–D) αIIbβ3-CHO cells were transduced with an HIV vector encoding for EGFP, for EGFP-conjugated full-length vinculin, for the EGFP-conjugated N-terminal region of talin (EGFP-TalinN; aa 1–1072) and for the EGFP-conjugated vinculin head domain (EGFP-Vin (1–880); aa 1–880). (B) The expression levels of the target proteins were confirmed by immunoblotting with an anti-GFP antibody. (C) PAC-1 binding after transduction in the presence or absence of 1 mM GRGDS was assessed by flow cytometry. The data are representative of at least three independent experiments. (D) Columns and error bars represent the mean ± SD of PAC-1 binding ($n = 3$–6). Differences between the two groups were analyzed statistically using Student's t test.

active form that binds to PAC-1 spontaneously [13]. The α6Bβ3-CHO cells were transduced with the indicated LentiLox vectors and the protein expressions were determined by immunoblotting. As shown in Fig. 1A, the expression levels of vinculin and talin-1 were significantly inhibited by expression of their specific shRNA sequences. We further confirmed that EGFP and αIIbβ3 expression remained unchanged in these experiments (Fig. 1B). Although binding of PAC-1 to α6Bβ3-CHO cells was significantly inhibited by loss of vinculin, the inhibitory effect was much weaker than that produced by silencing of talin-1 (Fig. 1C andD). These data indicate that loss of vinculin marginally affected the energy-dependent activation of αIIbβ3.

Next, we examined whether vinculin itself induced native αIIbβ3 activation. We created cDNAs for three EGFP-fusion proteins as follows: EGFP-conjugated N-terminal region of mouse talin-1 (EGFP-TalinN; aa 1–1072); EGFP-conjugated full-length vinculin (EGFP-vinculin) and an EGFP-conjugated N-terminal region of vinculin containing the head and neck domains (EGFP-Vin (1–880); aa 1–880) (Fig. 2A). The DNA fragments encoding these EGFP-fusion proteins driven by the CMV promoter were inserted individually into the HIV vector (Fig. 2A). The expression of the N-terminal region of talin (aa 1–1072) activated the native αIIbβ3 expressed on αIIbβ3-CHO cells (Fig. 2C and D), as reported [14]. Interestingly, the expression of EGFP-Vin (1–880), but not full-length EGFP-vinculin, significantly induced the activation of αIIbβ3 expressed on αIIbβ3-CHO cells (Fig. 2C and D).

To further assess the molecular mechanisms by which vinculin activates αIIbβ3, we created other fusion constructs to EGFP derivatives as follows: head domain of vinculin (EGFP-Vin (1–258); aa 1–258); C-terminal tail region of vinculin (EGFP-Vin (881–1066); aa 881–1066) and a constitutively active form of vinculin bearing mutations that inhibit the head–tail association (EGFP-Vin (T 12)) (Fig. 3A) [3]. PAC-1 binding to CHO cells expressing native αIIbβ3 was significantly increased by the expression of EGFP-Vin (1–880) but also EGFP-Vin (1–258) and EGFP-Vin (T 12), but was not affected by the expression of EGFP-Vin (881–1066) (Fig. 3C). The increase in PAC-1 binding elicited by EGFP-Vin (1–880) was much higher than those elicited by EGFP-Vin (1–258) or EGFP-Vin (T 12) (Fig. 3C). These data suggest that the activated form of vinculin can increase the ligand-binding capacity of αIIbβ3.

3.2. Talin-1 is required for vinculin-mediated integrin αIIbβ3 activation

Because vinculin is unable to interact constitutively with integrin cytoplasmic tails, we focused on the role of talin-1 in vinculin-elicited αIIbβ3 activation. The αIIbβ3-CHO cells transduced with HIV vectors expressing EGFP-TalinN or EGFP-Vin (1–880) were simultaneously transduced with LentiLox vectors containing the control (random), talin-1 (Talin-A) or vinculin (Vin-B) shRNA sequences, in which the CMV promoter and EGFP sequence in LentiLox had been removed (Fig. 4A). As shown in Fig. 4B, we confirmed the respective disappearances of the EGFP-conjugated Talin-N and vinculin constructs mediated by the Talin-A and Vin-B shRNA sequences using flow cytometry. Notably, PAC-1 binding by the vinculin head domain was significantly abolished by the silencing of talin-1 (Fig. 4C), suggesting that talin-1 is required for vinculin-induced integrin αIIbβ3 activation. On the other hand, talin-dependent activation of αIIbβ3 was not affected by the loss of vincluin (Fig. 4C).

3.3. Vinculin is not required for the spreading of α6Bβ3-CHO cells

Finally, we investigated whether vinculin is involved in outside-in signaling of αIIbβ3 by examining cell spreading on a fibrinogen substrate. We employed α6Bβ3-CHO cells treated with PT 25-2, a

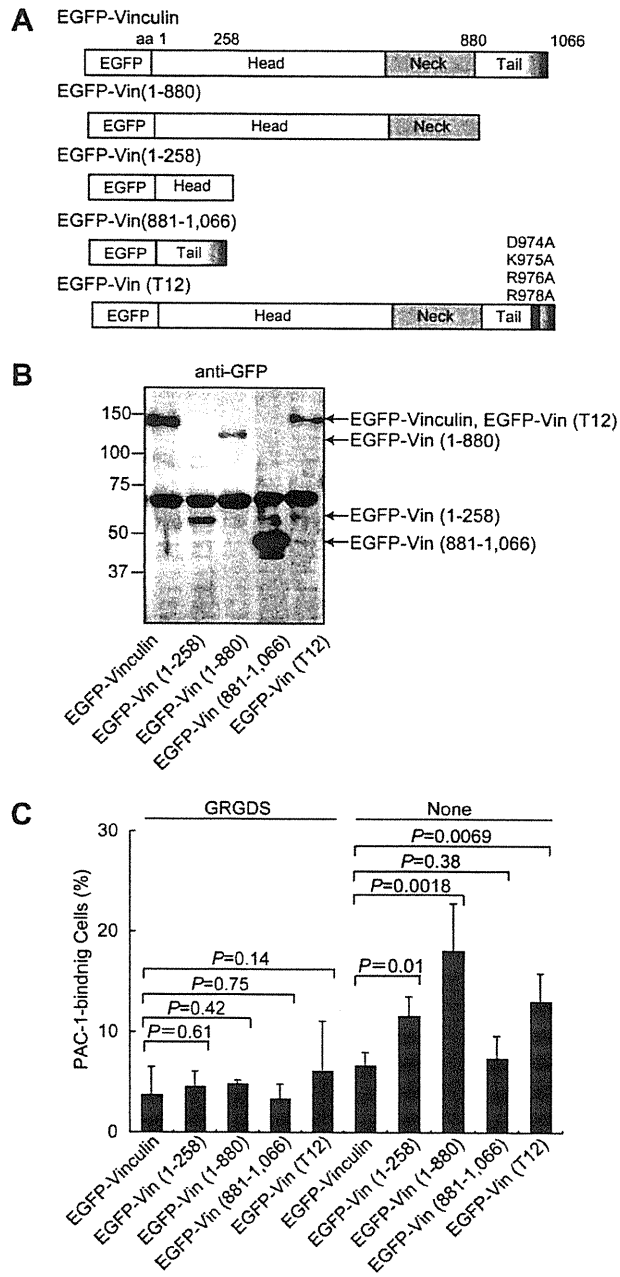

Fig. 3. Effects of various mutant forms of vinculin on the activation of integrin αIIbβ3 in CHO cells. (A) Schematic representations of the vinculin constructs expressed as fusion constructs with EGFP derivatives in αIIbβ3-CHO cells using HIV vectors. (B) The protein expression levels after transduction of the HIV vectors were confirmed by immunoblotting using an anti-GFP antibody. (C) PAC-1 binding after transduction with the indicated HIV vectors in the presence or absence of 1 mM GRGDS was assessed by flow cytometry. Columns and error bars represent the mean ± SD of PAC-1 binding ($n = 4$). Differences between the two groups were analyzed statistically using Student's t test.

mAb that induces αIIbβ3 activation, to completely remove the role of inside-out signaling. PAC-1 binding to α6Bβ3-CHO cells was significantly enhanced by the addition of PT 25-2, even in the absence of talin-1 (Supplementary Fig. 1A and B). Under the same conditions, silencing of talin-1 failed to induce cell spreading on fibrinogen (Supplementary Fig. 1A and B), confirming the role of talin-1 in αIIbβ3 outside-in signaling. On the other hand, loss of vinculin in α6Bβ3-CHO cells only marginally affected cell spreading (Supplementary Fig. 1A and B).

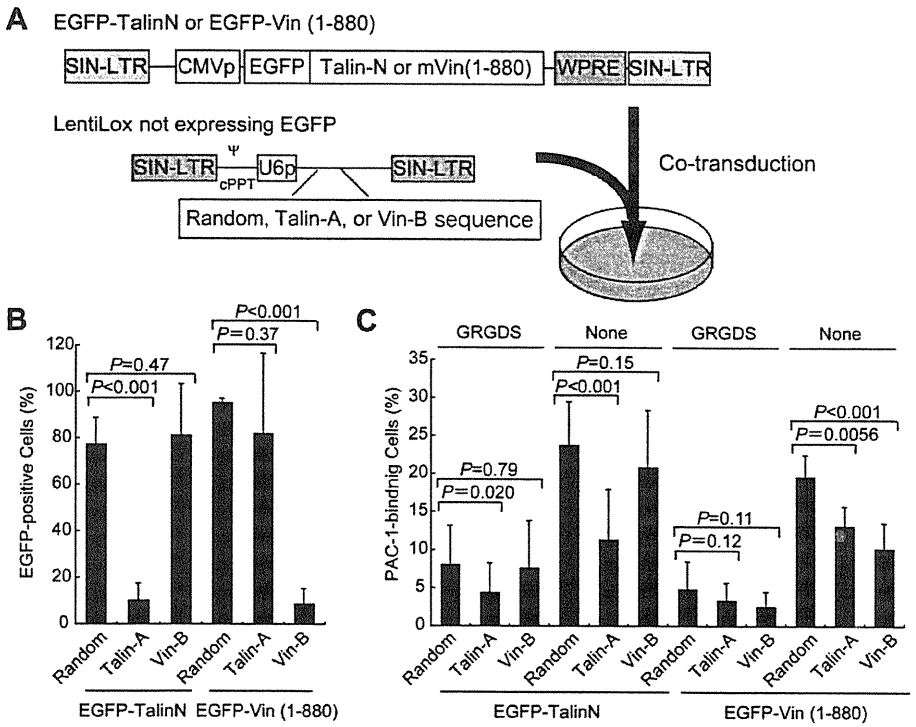

Fig. 4. Talin-1 is required for integrin activation elicited by vinculin. (A) αIIbβ3-CHO cells transduced with HIV vectors expressing EGFP-TalinN or EGFP-Vin (1–880) were simultaneously infected with the indicated LentiLox vectors (not expressing EGFP). (B) PAC-1 binding after transduction in the presence or absence of 1 mM GRGDS was assessed by flow cytometry. Columns and error bars represent the mean ± SD of EGFP expression after the transduction. The expression of each EGFP-fusion protein was reduced significantly by the corresponding shRNA sequence. (C) Columns and error bars represent the mean ± SD of PAC-1 binding ($n = 4$). Differences between the two groups were analyzed statistically using Student's t test.

4. Discussion

Although vinculin is used as a general marker for integrin-mediated formation of focal adhesion complexes, its importance in modulating the ligand-binding capacities of integrins has not been well addressed. The signal transduction pathways that lead to conformational changes of integrins are referred to as "inside-out signaling" pathways [7]. Cellular control of integrin activation requires transmission of a signal from the small cytoplasmic tails to the large extracellular domains. To date, more than 20 proteins have been identified to interact with either one or both cytoplasmic tails participating in inside-out signaling of αIIbβ3 [15]. Among these, it is well established that the binding of talin to β-integrin tails represents a final common step in integrin activation [16]. Kindlins and integrin-linked kinase (ILK) have now emerged as novel factors for integrin activation that can directly associate with β-integrin tails [12,17–19]. Although vinculin cannot bind directly to integrin cytoplasmic tails, our data suggest that it may have a role for inside-out signaling of αIIbβ3.

In the present study, the activation status of vinculin was found to be essential for increasing its affinity for integrins, because all the constructs that inhibited the intramolecular interaction also induced PAC-1 binding to αIIbβ3. Vinculin comprises three major domains that interact with other molecules, namely an N-terminal head domain, a flexible proline-rich neck domain (hinge) and a C-terminal tail domain [4,20]. The head domain can bind to talin and α-actinin, while the proline-rich region within the neck domain binds to vasodilator-stimulated phosphoprotein, vinexin, ponsin and the Arp2/3 complex [1]. Furthermore, other molecules including paxillin, F-actin and phosphatidylinositol (4,5)-bisphosphate (PIP_2) were reported to bind to the tail domain [1]. The crystal structure of vinculin has recently provided a molecular explanation for the two conformations. In the closed state (inactivated form), the tail domain interacts with the N-terminal head domain, burying most of the binding sites for other molecules within vinculin [4,21,22]. Our data revealed that constitutively activated forms of vinculin that cannot assume the autoinhibited conformation induced the ligand-binding capacity of αIIbβ3. Of note, a truncated form containing the head and neck domains (aa 1–880) displayed more powerful αIIbβ3 activation than the activation status induced by the expression of the head domain only or the T 12 mutant form. These data suggest that the head and neck domains of vinculin both play important roles in increasing its ligand-binding capacity, while the tail domain's interactions with PIP_2 and/or F-actin negatively regulate vinculin to activate integrin inside-out signaling.

The molecular mechanism by which vinculin modulates integrin affinity seems to differ from those of talin-1 and ILK, because loss of vinculin marginally affected the ligand-binding capacity of αB6β3, a constitutively active form of αIIbβ3. One possible explanation is that vinculin stabilizes talin-mediated integrin activation after ligand binding. Talin was reported to activate vinculin by provoking helical bundle conversion [22]. Recently, it was reported that increased tension at focal adhesions stretches the talin rod domain, thereby triggering conformational changes that reveal new vinculin-binding sites in talin [23]. These alterations might enhance the affinities of integrins and enable stronger binding of the integrins to the extracellular matrix [24]. In support of this idea, vinculin-null cells can form focal adhesion complexes, but are less adherent and more motile, suggesting that vinculin stabilizes the interactions of integrins and their ligands [5,25].

During the preparation of this manuscript, successful generation of megakaryocyte/platelet lineage-specific vinculin-deficient mice by breeding *Vcl fl/fl* mice with *Pf4-Cre* mice was reported

[26]. Although the tail bleeding times were prolonged in mice producing vinculin-deficient platelets, platelet functions including platelet aggregation and adhesion were similar to wild-type mice [26]. These phenotypes differ from those obtained from talin-1- or kindlin-3-deficient platelets [18,27,28] and these results could not fully explain the mechanism whereby the bleeding time is prolonged in vinculin-deficient mice. Considering that the activation status of vinculin proved important to increase the ligand binding of αIIbβ3 in this study, the mechanism to activate vinculin might exist at the site of vascular injury *in vivo*, thereby stabilizing thrombus formation.

In a study of vinculin-deficient embryos, vinculin was shown to be necessary for normal neural and cardiac development [5]. Furthermore, transgenic mice with cardiac myocyte-specific deletion of the gene for vinculin exhibit sudden death and dilated cardiomyopathy [29]. Although these abnormalities are supposed to result from perturbation of integrin-dependent cell functions, the effects of specific functions of vinculin that are independent of integrins cannot be ruled out. We recently reported that vinculin also plays roles in hematopoietic stem cell reconstitution independently of its integrin function [10]. We are interested in further investigating the integrin-independent functions of vinculin and corresponding experiments are now under way in our laboratory.

Acknowledgments

We would like to acknowledge Dr. K. Eto (Tokyo University) for very helpful discussions. We also thank Ms. N. Matsumoto and Mr. M. Ito for their excellent technical assistance. This study was supported by grants from the Mitsubishi Pharma Research Foundation, Grants-in-Aid for Scientific Research (20591155, 21591249 and 21790920) and the Support Program for Strategic Research Infrastructure from the Japanese Ministry of Education and Science, and by Health, Labor and Science Research Grants for Research on HIV/AIDS and Research on Intractable Diseases from the Japanese Ministry of Health, Labor and Welfare.

Appendix A. Supplementary material

Supplementary data associated with this article can be found, in the online version, at doi:10.1016/j.bbrc.2010.08.056.

References

[1] W.H. Ziegler, R.C. Liddington, D.R. Critchley, The structure and regulation of vinculin, Trends Cell Biol. 16 (2006) 453–460.
[2] W.H. Ziegler, A.R. Gingras, D.R. Critchley, J. Emsley, Integrin connections to the cytoskeleton through talin and vinculin, Biochem. Soc. Trans. 36 (2008) 235–239.
[3] J.D. Humphries, P. Wang, C. Streuli, B. Geiger, M.J. Humphries, C. Ballestrem, Vinculin controls focal adhesion formation by direct interactions with talin and actin, J. Cell Biol. 179 (2007) 1043–1057.
[4] C. Bakolitsa, D.M. Cohen, L.A. Bankston, A.A. Bobkov, G.W. Cadwell, L. Jennings, D.R. Critchley, S.W. Craig, R.C. Liddington, Structural basis for vinculin activation at sites of cell adhesion, Nature 430 (2004) 583–586.
[5] W. Xu, H. Baribault, E.D. Adamson, Vinculin knockout results in heart and brain defects during embryonic development, Development 125 (1998) 327–337.
[6] J.S. Bennett, Structure and function of the platelet integrin alphaIIbbeta3, J. Clin. Invest. 115 (2005) 3363–3369.
[7] B.S. Coller, S.J. Shattil, The GPIIb/IIIa (integrin alphaIIbbeta3) odyssey: a technology-driven saga of a receptor with twists, turns, and even a bend, Blood 112 (2008) 3011–3025.
[8] M. Tokuhira, M. Handa, T. Kamata, A. Oda, M. Katayama, Y. Tomiyama, M. Murata, Y. Kawai, K. Watanabe, Y. Ikeda, A novel regulatory epitope defined by a murine monoclonal antibody to the platelet GPIIb–IIIa complex (alpha IIb beta 3 integrin), Thromb. Haemost. 76 (1996) 1038–1046.
[9] T. Ohmori, Y. Kashiwakura, A. Ishiwata, S. Madoiwa, J. Mimuro, Y. Sakata, Silencing of a targeted protein in in vivo platelets using a lentiviral vector delivering short hairpin RNA sequence, Arterioscler Thromb. Vasc. Biol. 27 (2007) 2266–2272.
[10] T. Ohmori, Y. Kashiwakura, A. Ishiwata, S. Madoiwa, J. Mimuro, Y. Furukawa, Y. Sakata, Vinculin is indispensable for repopulation by hematopoietic stem cells, independent of integrin function, J. Biol. Chem. (2010), [Epub ahead of print].
[11] T. Ohmori, J. Mimuro, K. Takano, S. Madoiwa, Y. Kashiwakura, A. Ishiwata, M. Niimura, K. Mitomo, T. Tabata, M. Hasegawa, K. Ozawa, Y. Sakata, Efficient expression of a transgene in platelets using simian immunodeficiency virus-based vector harboring glycoprotein Ibalpha promoter: in vivo model for platelet-targeting gene therapy, Faseb J. 20 (2006) 1522–1524.
[12] S. Honda, H. Shirotani-Ikejima, S. Tadokoro, Y. Maeda, T. Kinoshita, Y. Tomiyama, T. Miyata, Integrin-linked kinase associated with integrin activation, Blood 113 (2009) 5304–5313.
[13] T.E. O'Toole, Y. Katagiri, R.J. Faull, K. Peter, R. Tamura, V. Quaranta, J.C. Loftus, S.J. Shattil, M.H. Ginsberg, Integrin cytoplasmic domains mediate inside-out signal transduction, J. Cell Biol. 124 (1994) 1047–1059.
[14] D.A. Calderwood, R. Zent, R. Grant, D.J. Rees, R.O. Hynes, M.H. Ginsberg, The talin head domain binds to integrin beta subunit cytoplasmic tails and regulates integrin activation, J. Biol. Chem. 274 (1999) 28071–28074.
[15] B. Nieswandt, D. Varga-Szabo, M. Elvers, Integrins in platelet activation, J. Thromb. Haemost. 7 (Suppl. 1) (2009) 206–209.
[16] S. Tadokoro, S.J. Shattil, K. Eto, V. Tai, R.C. Liddington, J.M. de Pereda, M.H. Ginsberg, D.A. Calderwood, Talin binding to integrin beta tails: a final common step in integrin activation, Science 302 (2003) 103–106.
[17] Y.Q. Ma, J. Qin, C. Wu, E.F. Plow, Kindlin-2 (Mig-2): a co-activator of beta3 integrins, J. Cell Biol. 181 (2008) 439–446.
[18] M. Moser, B. Nieswandt, S. Ussar, M. Pozgajova, R. Fassler, Kindlin-3 is essential for integrin activation and platelet aggregation, Nat. Med. 14 (2008) 325–330.
[19] K.L. Tucker, T. Sage, J.M. Stevens, P.A. Jordan, S. Jones, N.E. Barrett, R. St-Arnaud, J. Frampton, S. Dedhar, J.M. Gibbins, A dual role for integrin-linked kinase in platelets: regulating integrin function and alpha-granule secretion, Blood 112 (2008) 4523–4531.
[20] W. Eimer, M. Niermann, M.A. Eppe, B.M. Jockusch, Molecular shape of vinculin in aqueous solution, J. Mol. Biol. 229 (1993) 146–152.
[21] T. Izard, C. Vonrhein, Structural basis for amplifying vinculin activation by talin, J. Biol. Chem. 279 (2004) 27667–27678.
[22] T. Izard, G. Evans, R.A. Borgon, C.L. Rush, G. Bricogne, P.R. Bois, Vinculin activation by talin through helical bundle conversion, Nature 427 (2004) 171–175.
[23] A. del Rio, R. Perez-Jimenez, R. Liu, P. Roca-Cusachs, J.M. Fernandez, M.P. Sheetz, Stretching single talin rod molecules activates vinculin binding, Science 323 (2009) 638–641.
[24] M.A. Schwartz, Cell biology. The force is with us, Science 323 (2009) 588–589.
[25] W.H. Goldmann, R. Galneder, M. Ludwig, W. Xu, E.D. Adamson, N. Wang, R.M. Ezzell, Differences in elasticity of vinculin-deficient F9 cells measured by magnetometry and atomic force microscopy, Exp. Cell Res. 239 (1998) 235–242.
[26] J.V. Mitsios, N. Prevost, A. Kasirer-Friede, E. Gutierrez, A. Groisman, C.S. Abrams, Y. Wang, R.I. Litvinov, A. Zemljic-Harpf, R.S. Ross, S.J. Shattil, What is vinculin needed for in platelets?, J. Thromb. Haemost. (2010), [Epub ahead of print].
[27] B.G. Petrich, P. Marchese, Z.M. Ruggeri, S. Spiess, R.A. Weichert, F. Ye, R. Tiedt, R.C. Skoda, S.J. Monkley, D.R. Critchley, M.H. Ginsberg, Talin is required for integrin-mediated platelet function in hemostasis and thrombosis, J. Exp. Med. 204 (2007) 3103–3111.
[28] B. Nieswandt, M. Moser, I. Pleines, D. Varga-Szabo, S. Monkley, D. Critchley, R. Fassler, Loss of talin1 in platelets abrogates integrin activation, platelet aggregation, and thrombus formation in vitro and in vivo, J. Exp. Med. 204 (2007) 3113–3118.
[29] A.E. Zemljic-Harpf, J.C. Miller, S.A. Henderson, A.T. Wright, A.M. Manso, L. Elsherif, N.D. Dalton, A.K. Thor, G.A. Perkins, A.D. McCulloch, R.S. Ross, Cardiac-myocyte-specific excision of the vinculin gene disrupts cellular junctions, causing sudden death or dilated cardiomyopathy, Mol. Cell Biol. 27 (2007) 7522–7537.

THE JOURNAL OF BIOLOGICAL CHEMISTRY VOL. 285, NO. 41, pp. 31763–31773, October 8, 2010

Vinculin Is Indispensable for Repopulation by Hematopoietic Stem Cells, Independent of Integrin Function*[S]

Received for publication, December 24, 2009, and in revised form, July 13, 2010 Published, JBC Papers in Press, July 27, 2010, DOI 10.1074/jbc.M109.099085

Tsukasa Ohmori[‡1], Yuji Kashiwakura[‡], Akira Ishiwata[‡], Seiji Madoiwa[‡], Jun Mimuro[‡], Yusuke Furukawa[§], and Yoichi Sakata[‡2]

From the [‡]Research Division of Cell and Molecular Medicine and the [§]Division of Stem Cell Regulation, Center for Molecular Medicine, Jichi Medical University, Tochigi 329-0498, Japan

Vinculin is a highly conserved actin-binding protein that is localized in integrin-mediated focal adhesion complexes. Although critical roles have been proposed for integrins in hematopoietic stem cell (HSC) function, little is known about the involvement of intracellular focal adhesion proteins in HSC functions. This study showed that the ability of c-Kit$^+$Sca1$^+$Lin$^-$ HSCs to support reconstitution of hematopoiesis after competitive transplantation was severely impaired by lentiviral transduction with short hairpin RNA sequences for vinculin. The potential of these HSCs to differentiate into granulocytic and monocytic lineages, to migrate toward stromal cell-derived factor 1α, and to home to the bone marrow *in vivo* were not inhibited by the loss of vinculin. However, the capacities to form long term culture-initiating cells and cobblestone-like areas were abolished in vinculin-silenced c-Kit$^+$Sca1$^+$Lin$^-$ HSCs. In contrast, adhesion to the extracellular matrix was inhibited by silencing of talin-1, but not of vinculin. Whole body *in vivo* luminescence analyses to detect transduced HSCs confirmed the role of vinculin in long term HSC reconstitution. Our results suggest that vinculin is an indispensable factor determining HSC repopulation capacity, independent of integrin functions.

The development and maintenance of hematopoietic stem cells (HSCs),[3] which can self-renew and differentiate into all hematopoietic blood cell lineages, are thought to depend on their interactions with the microenvironment, referred to as their "niche" (1, 2). Direct molecular interactions of HSCs in the bone marrow (BM) through N-cadherin and Tie2 reportedly sustain HSC maintenance and self-renewal (3, 4). Although the importance of integrins and their ligand interactions in the hematopoietic niche are not fully understood, critical roles have been proposed for integrins in HSC functions. HSCs mainly express integrins α4, α5, and α6, which can associate with integrin β1 (5). Integrin β1-null HSCs fail to engraft in irradiated recipient mice, because of sequestration of the HSCs into the circulation (failure of HSCs to home to the BM and spleen) (6). Conditional ablation of integrin α4 in hematopoietic cells results in sustained and significant increases in circulating progenitors (7), whereas administration of a function-blocking antibody (Ab) or blocking peptide against integrin α4 reduces HSC homing and leads to HSC release into the blood (8, 9). Furthermore, integrin α4β1-mediated attachment of HSCs to fibronectin promotes their proliferation and survival (10).

Integrins are heterodimeric receptors formed by noncovalent associations between α and β subunits. There are at least 24 different combinations of subunits, each of which can bind to a specific ligand, including extracellular matrix components (ECM) and soluble ligands, after their activation (11). The conformation of integrins is tightly controlled through interactions between cytoplasmic focal adhesion proteins and the integrin cytoplasmic tails, which regulate the transition from a low to a high affinity ligand-binding state (12, 13). Among these integrin-associated proteins, talin, the kindlin family, and integrin-linked kinase have emerged as essential for integrin activation and linkage to the actin cytoskeleton (14–18).

Vinculin is a highly conserved actin-binding protein that is frequently used as a marker for integrin-mediated cell-ECM interactions (19). Although vinculin itself does not bind directly to integrins, it is thought to play key roles in focal adhesion assembly and cell adhesion (19). The crystal structure of vinculin reveals that its N-terminal head domain forms a complex with the rod domain of talin, which contains three vinculin-binding sites (20, 21). Vinculin is autoinhibited by intramolecular interactions (22), but its conformation can be changed by interactions with talin and actin, making it functionally active (23). Although numerous studies have investigated the structure of vinculin and its associations with talin and other cytoskeletal proteins, the precise role of these cytoskeletal proteins in directly modulating the function of HSCs remains to be elucidated. In this study, we focused on the involvement of two well known focal adhesion proteins, vinculin and talin-1, in HSC function, and provide the first evidence that vinculin is

* This work was supported by Grants from the Mitsubishi Pharma Research Foundation; Grants-in-Aid for Scientific Research (20591155, 21591249, and 21790920) and the Support Program for Strategic Research Infrastructure from the Japanese Ministry of Education and Science; and Health, Labour and Science Research Grants for Research on HIV/AIDS and Research on Intractable Diseases from the Japanese Ministry of Health, Labour and Welfare.

[S] The on-line version of this article (available at http://www.jbc.org) contains supplemental text, Table S1, and Figs. S1–S5.

[1] To whom correspondence may be addressed: Yakushiji 3311-1 Shimotsuke, Tochigi 329-0498, Japan. Tel.: 81-285-58-7397; Fax: 81-285-44-7817; E-mail: tohmori@jichi.ac.jp.

[2] To whom correspondence may be addressed: Yakushiji 3311-1 Shimotsuke, Tochigi 329-0498, Japan. Tel.: 81-285-58-7397; Fax: 81-285-44-7817; E-mail: yoisaka@jichi.ac.jp.

[3] The abbreviations used are: HSC, hematopoietic stem cell; BM, bone marrow; Ab, antibody; ECM, extracellular matrix; EGFP, enhanced GFP; MOI, multiplicity of infection; KSL, c-Kit$^+$Sca1$^+$Lineage$^-$; TPO, thrombopoietin; CFU-GM, colony-forming units of granulocytes/macrophages; CFU-G, colony-forming units of granulocytes; LTC-IC, long term culture-initiating cells.

involved in HSC repopulation through an integrin-independent mechanism.

EXPERIMENTAL PROCEDURES

An expanded "Methods" section including detailed information on materials, bone marrow transplantation, RT-PCR, and immunoblotting is provided in the supplemental materials.

Construction of Lentiviral Vectors and Virus Production—The gene transfer vector pLL3.7 (LentiLox) for constructing replication-defective self-inactivating HIV lentiviral vectors expressing shRNA sequences was purchased from ATCC (Manassas, VA) (see Fig. 1*A*) (24). Putative shRNA sequences were designed using the web software provided by Dharmacon RNA Technologies. Each shRNA sequence was cloned into the HpaI and XhoI sites of pLL3.7 (see Fig. 1*A* and supplemental Table S1) (24). The control (random) and talin-1 (Talin-A) shRNA sequences have been reported previously (25). We designed three shRNA sequences for mouse vinculin, designated Vin-B, Vin-C, and Vin-D, and found that ectopic expression of mouse vinculin in HEK293 cells was significantly inhibited by cotransfection with the constructs expressing the Vin-B and Vin-C shRNA sequences (data not shown). We therefore selected the Vin-B and Vin-C sequences for use in this study. The lentiviral vectors were essentially generated as described previously (26). The vector titers of LentiLox carrying enhanced green fluorescent protein (EGFP) were measured by infection of 1×10^5 UT-7/TPO cells (a megakaryoblastic cell line). EGFP expression was measured by FACS analysis at 48 h after transduction. Typically, 1 μl of concentrated vector solution was able to transduce EGFP in 50–60% of the cells, and the vector titers for UT-7/TPO cells were considered to be $5–6 \times 10^7$ cells/ml. Because the vector titers against HEK293 cells were much higher than those against UT-7/TPO cells, the multiplicity of infections (MOIs) used in this study were lower than those in our previous studies (25, 26).

Isolation of c-Kit$^+$Sca1$^+$Lin$^-$ (KSL) HSCs and Competitive Reconstitution Assay—C57BL/6 mice (Ly5.2) and C57BL/6 mice congenic for the Ly5 locus (Ly5.1) were purchased from Japan SLC (Shizuoka, Japan) and Sankyo-Lab Service (Tsukuba, Japan), respectively. All of the animal procedures were approved by the Institutional Animal Care and Concern Committee of Jichi Medical University, and animal care was performed in accordance with the committee guidelines. BM cells were depleted of cells expressing the cell lineage markers B220, CD3e, CD11b, Gr-1, and Ter-119 (biotin-conjugated mouse lineage panel; BD Biosciences Co., San Jose, CA) by magnetic cell sorting using streptavidin microbeads (Miltenyi Biotec, Gladbach, Germany) and a magnetic cell sorter (autoMACS™; Miltenyi Biotec). The remaining cells were sorted for KSL cells by FACS (FACSAria™ Cell Sorter; BD Biosciences) (see Fig. 1*B*). CD34^{low} KSL cells, comprising HSCs with long term BM repopulating ability, were defined as the lowest 20% of the KSL cell population in terms of CD34 expression. The isolated KSL cells were cultured in StemPro®-34 SFM medium (Invitrogen) supplemented with 100 ng/ml stem cell factor, 100 ng/ml TPO, 100 ng/ml IL-6, 100 ng/ml fms-like tyrosine kinase 3 ligand, and 200 ng/ml soluble IL-6 receptor for 16 h before lentiviral transduction. The cells were transduced with lentiviral vectors at a MOI of 20 in the presence of the same cytokines and polybrene (8 μg/ml). After the transduction with LentiLox vectors, EGFP expression was confirmed in at least 80% of the transduced KSL cells in the subsequent experiments (see Fig. 1*C*). When EGFP-positive cells comprised less than 80% of the cells, the EGFP-positive KSL cells were further sorted by FACS, and the sorted cells were then used in subsequent experiments on the following day.

Competitive reconstitution assays were performed using the Ly5 congenic mouse system. Recipient Ly5.2 mice (8–12 weeks of age) were irradiated with a single lethal dose of 9.5 grays (Gamma Cell; Norton International), followed by injection of 1×10^5 transduced KSL cells from Ly5.1 donor mice, together with 2×10^5 freshly isolated Ly5.2 unfractionated BM cells.

Colony-forming Cell Assays—Colony-forming cell assays were performed as described previously (27). Briefly, KSL cells were transduced with LentiLox vectors at a MOI of 20. Transduced cells (2×10^3) were then suspended in 1 ml of MethoCult™ M3231 medium (StemCell Technologies) supplemented with 20 ng/ml of mouse granulocyte macrophage-colony stimulating factor or 20 ng/ml of granulocyte-colony stimulating factor (for colony-forming units of granulocytes/macrophages (CFU-GM) or colony-forming units of granulocytes (CFU-G), respectively) and plated on 3.5-cm dishes. Colonies containing at least 30 cells on day 5 were counted under a microscope in five random fields at a magnification of ×40 by a blinded observer. The mean value from the duplicate experiments was treated as the result of a single independent experiment.

Cell Migration—Cell migration was assessed by a modified Boyden chamber assay using Costar Transwell® cell culture inserts (Corning Inc., Canton, NY) with polycarbonate filters, with 8-μm pores separating the upper and lower chambers. Transduced KSL cells were added to the upper chamber at a density of 1×10^5 cells/100 μl of DMEM/Ham's F-12 medium containing 1% fatty acid-free BSA and incubated for 4 h at 37 °C. The cells were allowed to migrate toward 100 ng/ml of stromal cell-derived factor 1α in the lower chamber. Following migration, the cells in the lower chamber were recovered by centrifugation and then lysed using 200 μl of CyQUANT® GR dye/cell lysis buffer (Invitrogen). The cell number was quantified by measuring the fluorescence with excitation at 480 nm and emission detection at 520 nm.

HSC Homing to the BM and Spleen—HSC homing assays were essentially performed as described previously (28, 29). Briefly, transduced KSL cells (1×10^5 cells) were injected into lethally irradiated recipient mice (9.5 grays). At 16–20 h after transplantation, the cells from femurs and spleen were harvested, and 50% of a femur and 10% of the spleen homogenate/dish were used for CFU-GM assays, as described above. The CFU-GM colonies were counted manually by a blinded observer and considered to represent homing KSL cells in the BM or spleen after transplantation. Two percent of KSL cells were directly assessed for CFU-GM assays in each experiment to estimate the total number of CFU-GM colonies derived from the transplanted KSL cells. The mean values of duplicate experiments were calculated. The number of recovered CFU-GM was corrected to represent the whole BM, based on the estimate

that one femur represents 5.9% of the total BM (28, 29). The data are presented as the percentages of homing KSL cells; the total number of CFU-GM colonies from the BM or spleen was divided by the estimated number of CFU-GM colonies from injected KSL cells (number of CFU-GM from 2% of KSL cells multiplied by 50). One mouse for each experiment was irradiated but did not receive KSL cells to assess the number of residual host-derived CFU-GM; only 0–1 CFU-GM were observed in these BM and spleen samples.

Cell Proliferation Assay and Cell Cycle Analysis in Liquid Culture—Transduced KSL cells (1×10^4 cells) were suspended with 1 ml of StemPro-34 SFM medium supplemented with 50 ng/ml stem cell factor, 50 ng/ml TPO, 50 ng/ml IL-6, 50 ng/ml fms-like tyrosine kinase 3 ligand, and 100 ng/ml soluble IL-6 receptor in 12-well plates. The cell numbers were determined at specified time points using Flow-Count fluorospheres (Beckman Coulter, Miami, FL). All of the experiments were performed in triplicate, and the mean value was considered to represent the result of a single independent experiment. For cell cycle analysis, the cultured KSL cells ($1–2 \times 10^5$ cells) were suspended in 1 ml of StemPro-34 SFM medium supplemented with the same cytokine combination at 48–72 h after lentiviral transduction. The cells were incubated with 10 μl of 1 mM BrdU for 30 min. The cell cycle positions and active DNA synthetic activities of the cells were determined by analyzing the correlated expression of total DNA (7-aminoactinomycin D) and incorporated BrdU levels (anti-BrdU antibody) by FACS, in accordance with the manufacturer's instructions (BrdU flow kit; BD Biosciences).

Long Term Culture-initiating Cell (LTC-IC) Assay—LTC-IC assays were carried out using Myelocult™ M5300 medium (StemCell Technologies), according to the manufacturer's recommendations, with some modifications. Confluent C3H/10T1/2 cells (Health Science Research Resources Bank, Osaka, Japan) plated on 96-well plates were irradiated at 50 grays. Transduced KSL cells resuspended in 150 μl of Myelocult™ M5300 medium in limiting dilution solutions from 300 to 37.5 cells were seeded in 12 wells each and cultured for 4 weeks at 33 °C under 5% CO_2 with weekly half-medium changes. All of the cells were subsequently resuspended in 500 μl of methylcellulose medium (MethoCult™ M3434; StemCell Technologies), and CFU colonies were counted on day 12. The frequencies of LTC-IC were expressed as percentages of the positive wells (≥1 CFU/well) among 12 wells.

Cobblestone-like Area Forming Assay—Cobblestone-like area forming assays were essentially performed as reported previously (30). C3H/10T1/2 cells were cultured in 96-well plates and then irradiated with a single dose of 50 grays. Transduced KSL cells (62 cells) were suspended in 2 ml of Myelocult™ M5300 medium (StemCell Technologies). 150 μl of cell suspension was plated onto the irradiated C3H/10T1/2 cells and then cultured at 33 °C in 5% CO_2. Half of the medium was changed every week. The presence of cobblestone-like areas per well was manually assessed by a blinded observer at 28 days after seeding. The frequency of positive wells (containing one or more cobblestone areas) was expressed as a percentage of the positive wells among 12 wells.

Assessment of Transplanted KSL Cell Fates by Bioluminescence Studies—The fates of transduced KSL cells in identical recipient mice *in vivo* were assessed using bioluminescence imaging to assess directly the luciferase activities derived from the transduced KSL cells. KSL cells (Ly5.1) were transduced with LentiLox vectors expressing luciferase (instead of EGFP) and then transplanted into lethally irradiated recipient mice. Luciferase activities derived from the KSL cells were determined after anesthetizing the mice with isoflurane and intraperitoneally injecting them with the luciferin substrate (1.5 mg/body). Photons transmitted through the body were collected for a specified length of time and analyzed using an IVIS® Imaging System and Living Image software (Xenogen Corp., Alameda, CA). Quantitative data were expressed as photon units (photons/s). To confirm the transduction efficacies of KSL cells, the transduced KSL cells were directly assessed by the addition of the luciferin substrate (300 μg/ml) before transplantation, and the bioluminescence activity was measured for 3 min.

Cell Adhesion and Immunofluorescence Microscopy—Twenty-four-well tissue culture plates were coated with 10 μg/ml of fibronectin (Sigma-Aldrich) for 16 h at 4 °C or for 2 h at room temperature. After blocking of the plates with 2% BSA, 1×10^5 transduced KSL cells were suspended in 250 μl of StemPro-34 SFM medium, added to the plates with or without 2 mM EDTA or 2 mM $MnCl_2$, and incubated for 3 h. After washing with PBS, the numbers of adherent cells were quantified by the fluorescence of the CyQUANT® GR dye (Invitrogen), as described above. To observe adherent KSL cells by microscopy, dishes (4-well Lab-Tek® Chamber Slide™) were coated with 10 μg/ml fibronectin for 16 h at 4 °C, washed twice with PBS, and blocked with 2% BSA for 1 h. Transduced KSL cells (2×10^4) were placed onto the fibronectin-coated dishes for 3 h at 37 °C. After washing twice with PBS, adherent cells were fixed with 3% paraformaldehyde in PBS for 40 min and then permeabilized with PBS containing 0.3% Triton X-100 and 5% donkey serum for 2 h. After washing with PBS, the cells were incubated with biotin-conjugated anti-GFP polyclonal Ab (1:200) (Abcam plc., Cambridge, UK) for 16 h at 4 °C, washed in PBS, and then incubated for 2 h with streptavidin conjugated with Alexa488 (1:200) (Molecular Probes). Actin filaments were detected by staining with 10 μg/ml rhodamine-conjugated phalloidin (Sigma-Aldrich). The samples were mounted in Vectashield with DAPI (Vector Laboratories) and observed by confocal microscopy (FV1000; Olympus, Tokyo, Japan). When indicated, the cell area was quantified using Image J Ver. 10.2 for Macintosh (National Institutes of Health, Bethesda, MD) by a blinded observer.

RESULTS

Lentiviral Vector-mediated shRNAs Efficiently Inhibit Expression of Target Proteins in KSL HSCs—A lentiviral vector, in which the U6 RNA polymerase III promoter drives the expression of an shRNA for the target protein and the CMV promoter drives EGFP expression, was applied to inhibit target protein expression in KSL HSCs (Fig. 1*A*; LentiLox). A nonspecific control shRNA (random sequence), an shRNA directed against mouse talin-1 (Talin-A sequence), and two independent

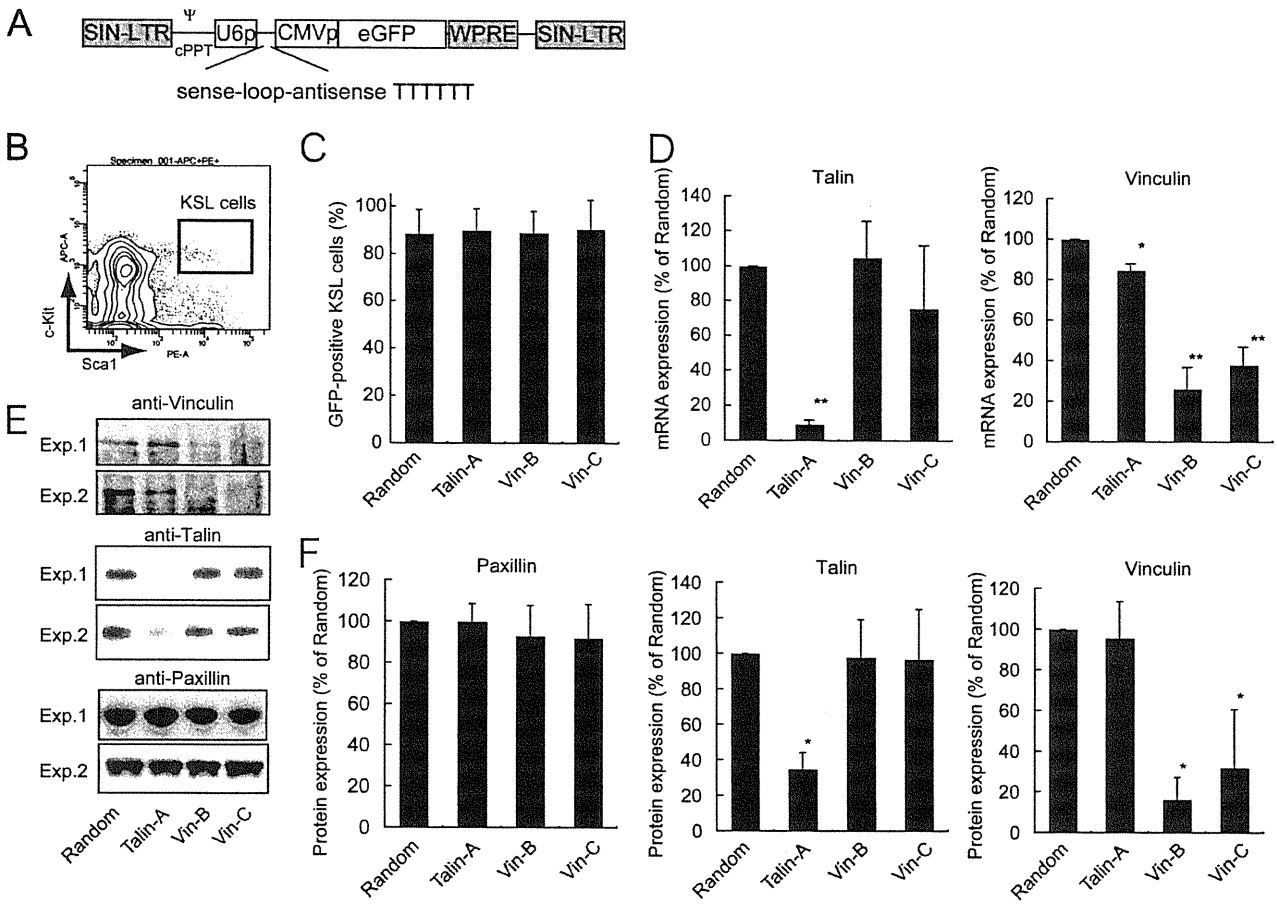

FIGURE 1. **Silencing of target protein and mRNA expression in KSL cells transduced with LentiLox vectors.** *A*, schematic presentation of the lentiviral vector (LentiLox). The shRNA sequences inserted into LentiLox are shown in supplemental Table S1. *B*, representative flow cytometric data for KSL cell sorting. *C*, expression of EGFP in KSL cells after transduction with LentiLox vectors expressing the indicated shRNA sequences at a MOI of 20 (n = 8–10). *D*, mRNA expression of talin (*left panel*) and vinculin (*right panel*) examined by real time quantitative PCR. The quantity was determined by dividing the copy number of the target sequence by that of the mouse glyceraldehyde-3-phosphate dehydrogenase sequence. Each value was expressed as a percentage relative to the value in the random shRNA experiment. The *columns* and *error bars* represent the means ± S.D. (n = 3). *E*, expression of vinculin, talin, and paxillin proteins in KSL cells transduced with the indicated LentiLox vectors examined by immunoblotting. Two representative data are shown. *F*, expression of paxillin (*left panel*), talin (*middle panel*), and vinculin (*right panel*) proteins was quantified using ImageJ software. Each value was expressed as a percentage relative to the value in the random experiment. The *columns* and *error bars* represent the means ± S.D. (n = 4). *, $p < 0.05$; **, $p < 0.01$, compared with the control experiment (random) under the same conditions (two-tailed Student's t test). *Exp.*, experiment.

shRNAs against mouse vinculin (Vin-B and Vin-C sequences) were designed. These sequences were confirmed to effectively inhibit ectopic expression of the target proteins in HEK293 cells (data not shown). The efficacies of these lentiviral constructs for inhibiting expression of the target mRNAs and proteins in HSCs were also examined. KSL HSCs isolated by FACS (Fig. 1*B*) were transduced with LentiLox vectors containing the random, Talin-A, Vin-B, or Vin-C sequences at MOIs of 20. We confirmed that the transduction efficiencies were as high as 80% of the KSL HSCs (Fig. 1*C*). The expression levels of the target proteins and their mRNAs in KSL cells were significantly inhibited by expression of the corresponding shRNA after transduction (Fig. 1*D–F* and supplemental Fig. S1). Vinculin expression in HSCs was inhibited more strongly by expression of the Vin-B sequence than by expression of the Vin-C sequence. Although levels of vinculin mRNA were marginally inhibited by the Talin-A sequence (~15%) (Fig. 1*D*), its protein levels were not significantly inhibited (Fig. 1*F*). The talin-1 shRNA sequence was confirmed to include five or more mismatch sequences for other mouse mRNAs in a BLAST search.

Expression of shRNAs against Vinculin Reduce Short Term Hematopoietic Engraftment—BM cells transduced with LentiLox vectors equipped with the random, Talin-A, Vin-B, or Vin-C shRNA sequences were transplanted to investigate the roles of vinculin and talin-1 in hematopoietic cell reconstitution after BM transplantation. After transplantation of the transduced BM cells at a MOI of 5, vinculin silencing resulted in fewer EGFP-positive peripheral blood cells, including CD45-positive white blood cells, red blood cells, and platelets, compared with control experiments (supplemental Fig. S2). Although talin-1-silencing in BM cells did reduce EGFP expression in peripheral blood cells, its inhibitory effects were weaker than those of vinculin silencing (supplemental Fig. S2). Despite the fact that not all blood cells were labeled with EGFP in this procedure, the method could still be used to determine the role of these proteins in HSC fate because the lentiviral vector used was able to simultaneously express the shRNA sequences and EGFP in identical transduced cells.

KSL cells transduced with the LentiLox vectors at a MOI of 20 were then transplanted together with nontransduced com-

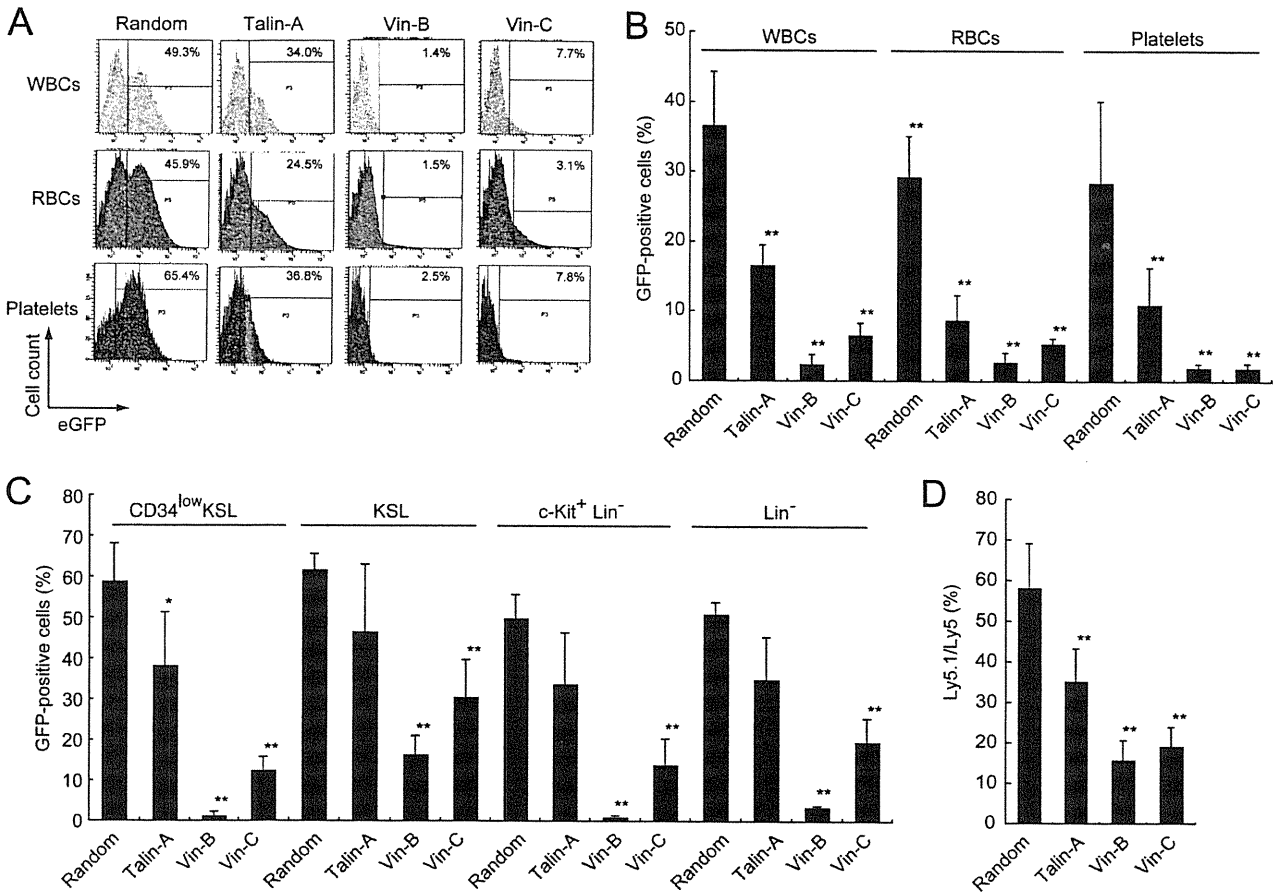

FIGURE 2. **Reconstitution capacities of EGFP-positive KSL cells transduced with LentiLox vectors.** Transduced KSL cells (1×10^5) isolated from Ly5.1 congenic mice together with nontransduced Ly5.2 BM cells (2×10^5) were transplanted into lethally irradiated recipient mice. EGFP expression in peripheral blood cells and BM cells was assessed at 1 month after transplantation. *A*, representative data for EGFP expression in CD45-positive white blood cells (*WBCs*), red blood cells (*RBCs*), and platelets in each experiment. *B*, quantification of EGFP expression in peripheral blood cells. The *columns* and *error bars* represent the means ± S.D. ($n = 6–11$). *C*, EGFP expression in the indicated BM cells. The *columns* and *error bars* represent the means ± S.D. ($n = 3–4$). *D*, chimerism after transplantation was calculated by the expression of Ly5.1-positive cells (%) among the total Ly5-positive white blood cells. The columns and *error bars* represent the means ± S.D. ($n = 6–11$). *, $p < 0.05$; **, $p < 0.01$, compared with the control experiment (random) under the same conditions (two-tailed Student's *t* test).

petitor cells into lethally irradiated recipient mice to examine the contribution of vinculin to HSC engraftment. As predicted based on the results of BM cell transplantation, vinculin silencing significantly reduced EGFP expression not only in white blood cells but also in platelets and red blood cells after transplantation of the transduced KSL HSCs (Fig. 2, *A* and *B*). Similar results were obtained at 2 months after transplantation (supplemental Fig. S3). EGFP expression in BM cells was also examined. c-Kit is expressed on HSCs and progenitor cells, whereas the KSL cell fraction contains more primitive stem cells (31). KSL cells were further subdivided according to their surface expression of CD34. $CD34^{low/-}$ $c\text{-}Kit^+Sca\text{-}1^+Lin^-$ ($CD34^{low}$KSL) cells are highly enriched for HSCs with long term marrow repopulating ability, whereas $CD34^+$ $c\text{-}Kit^+Sca\text{-}1^+Lin^-$ ($CD34^+$KSL) cells are progenitors with short term reconstitution capacity, suggesting that $CD34^{low}$KSL cells have a higher rank in the hematopoietic hierarchy than $CD34^+$KSL cells (32). The proportion of EGFP-positive cells was reduced by vinculin silencing not only in the progenitor fraction ($c\text{-}Kit^+Lin^-$ cells) but also in more primitive HSCs ($CD34^{low}$KSL cells), thus strengthening the initial hypothesis that vinculin controls HSC fate after transplantation (Fig. 2*C*). EGFP expression in Lin^+ BM cells was also inhibited after transplantation (supplemental Fig. S4). The chimerism percentage (Ly5.1/Ly5) in peripheral white blood cells after transplantation represents the relative reconstitution ability of transduced KSL cells (Ly5.1) compared with nontransduced competitor cells (Ly5.2). The Ly5.1/Ly5 ratio after transplantation was reduced by vinculin silencing (Fig. 2*D*). In contrast, the CFU-GM and CFU-G colony forming capacities of KSL cells were not affected by expression of the vinculin shRNA sequences (Fig. 3), suggesting that vinculin silencing did not affect the capacities of KSL cells to differentiate into granulocytic lineage cells. These results indicate that KSL HSCs lacking vinculin do not engraft efficiently after transplantation.

Frequencies of LTC-IC and Cobblestone-like Area Forming Capacities on BM Stromal Cells, but Not Homing to the BM, Are Impaired in Vinculin-silenced KSL HSCs—The observed reduction in HSC engraftment by vinculin silencing could be a consequence of a reduced ability of HSCs either to home to the BM or to reconstitute hematopoiesis (repopulating capacity of HSCs in the BM). The effect of vinculin silencing on HSC pro-

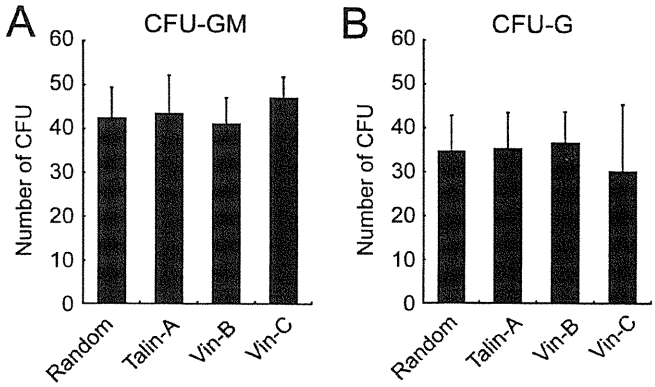

FIGURE 3. **Loss of vinculin does not impair CFU-GM or CFU-G colony formation.** KSL cells were transduced with the indicated LentiLox lentiviral vectors at a MOI of 20. Colony forming assays for GFU-GM and CFU-G were performed as described under "Experimental Procedures." *A* and *B*, the numbers of CFU-GM (*A*) and CFU-G (*B*) per 2×10^3 transduced KSL cells were assessed. The *columns* and *error bars* represent the means ± S.D. ($n = 3$). There were no significant differences between the groups (two-tailed Student's *t* test).

liferation was investigated to distinguish between these possibilities. Transduced KSL cells were cultured *in vitro* in serum-free medium containing a cytokine combination, and the cell numbers were assessed by FACS. As shown in Fig. 4*A*, cell proliferation in response to the cytokine combination was impaired in KSL HSCs expressing shRNA sequences for vinculin but not talin-1. The cell cycle of KSL cells in liquid culture was further investigated by FACS. As shown in Table 1, vinculin silencing was associated with an increase in the apoptotic cell fraction and a decrease of the proportion of S phase cells. These results suggest that the loss of vinculin, but not talin-1, affects cell survival through modulation of the cell cycle and induction of apoptosis in HSCs. LTC-IC and cobblestone-like area formation assays were used to examine the self-renewal and proliferative abilities of HSCs on a stromal cell layer. The number of LTC-IC in vinculin-silenced KSL cells was significantly reduced compared with controls (Fig. 4*B*). The loss of talin-1 also affected the frequencies of LTC-IC, although this effect was weaker than that of vinculin (Fig. 4*B*). In addition, cobblestone-like area-forming cells on the stromal cell layer were significantly abolished in KSL HSCs transduced with shRNA sequences for vinculin (Fig. 4*C*).

The homing capacities of the transduced KSL cells were also assessed. Although the expression of CXCR4 was unaffected by either talin-1 or vinculin silencing (Fig. 5*A*), the chemotactic responses of the transduced HSCs to mouse stromal cell-derived factor 1α *in vitro* were significantly higher in vinculin-silenced HSCs (Fig. 5*B*). In addition, the homing of KSL cells to the BM and spleen were unaffected by silencing of either vinculin or talin-1 (Fig. 5*C*). Taken together, these data suggest that vinculin is not required for HSC homing to the BM but is required for the self-renewal potential and proliferation of HSCs on BM stromal cell layers.

Visualization of Long Term in Vivo Hematopoietic Reconstitution of KSL HSCs—Long term HSC reconstitution after transplantation in identical recipient mice was investigated by replacing the *EGFP* gene in LentiLox with a *luciferase* gene, and luciferase activities derived from the transduced HSCs were observed directly using an IVIS® imaging system *in vivo* (Fig.

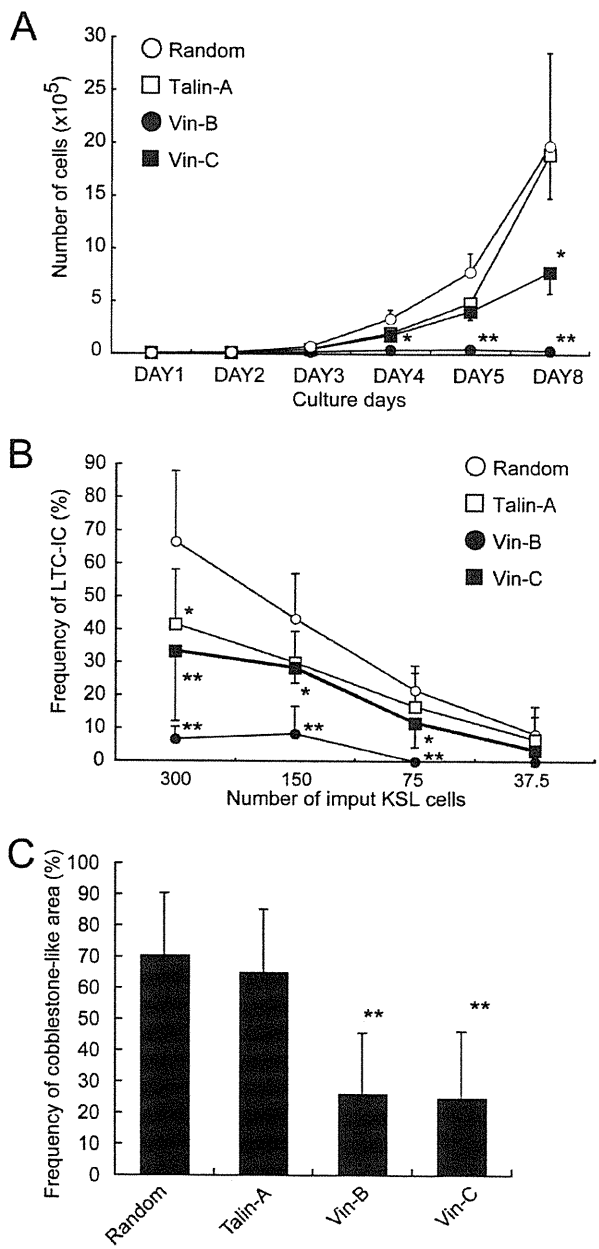

FIGURE 4. **Loss of vinculin impairs the frequencies of LTC-IC and cobblestone-like area-forming cells.** *A*, transduced KSL cells (1×10^4) were cultured in StemPro-34 SFM medium with a cytokine combination, as described under "Experimental Procedures." The cell numbers were quantified by FACS at the indicated time points. Values represent the means ± S.E. ($n = 5$). *B*, the frequencies of LTC-IC among KSL cells (300 to 37.5 cells) transduced with the indicated LentiLox vectors were examined as described under "Experimental Procedures." Values represent the means ± S.D. ($n = 5$). *C*, the frequency of cobblestone-like areas formed on irradiated C3H/10T1/2 cells was assessed at 28 days after seeding, as described under "Experimental Procedures." The *columns* and *error bars* represent the means ± S.D. ($n = 6$). *, $p < 0.05$; **, $p < 0.01$, compared with the control experiment (random) under the same conditions (two-tailed Student's *t* test).

6*A*). The luciferase activities of the transduced KSL cells were similar in all of the groups prior to transplantation (Fig. 6*B*). Luciferase activities derived from the transduced KSL cells were detected from 7 days after transplantation (Fig. 6*C*). Consistent with the data for the KSL cell homing experiments (Fig. 5*C*), early engraftment of HSCs lacking vinculin was achieved

TABLE 1
Quantitative cell cycle analysis of cultured KSL cells

Cell cycle	shRNA sequence	Means ± S.D. (n = 5)	p value
		%	
G_0/G_1 phase	Random	31.72 ± 3.53	
	Talin-A	34.12 ± 2.13	0.070
	Vin-B	35.02 ± 2.39	0.016[a]
	Vin-C	32.86 ± 4.21	0.46
S phase	Random	59.0 ± 3.29	
	Talin-A	51.5 ± 11.0	0.13
	Vin-B	45.9 ± 5.35	0.0013[a]
	Vin-C	55.3 ± 3.83	0.0384[a]
G_2/M phase	Random	2.82 ± 1.93	
	Talin-A	3.06 ± 1.71	0.66
	Vin-B	3.16 ± 1.59	0.64
	Vin-C	3.06 ± 1.67	0.76
Apoptotic cells	Random	5.44 ± 1.43	
	Talin-A	6.44 ± 3.73	0.49
	Vin-B	14.08 ± 3.71	0.0026[a]
	Vin-C	7.44 ± 1.41	0.0036[a]

[a] $p < 0.05$ compared with the control experiment (random) under the same conditions (Student's t test).

until 2 weeks after the transplantation (Fig. 6, *C* and *D*). The early luciferase activity derived from KSL cells expressing the Vin-B sequence was slightly attenuated (Fig. 6*C*). This was expected from the results of the cell proliferation experiments (Fig. 4*A*). It was notable that the luciferase activities derived from HSCs lacking vinculin seemed to gradually decrease, compared with the activities derived from control and talin-silenced cells (Fig. 6, *C* and *D*). These results support the idea that vinculin is an indispensable factor for HSC repopulation in the BM.

Loss of Talin-1, but Not Vinculin, Impairs Adhesion of KSL Cells to the ECM—The effect of vinculin silencing on HSC function, through integrin expression and adhesion to the ECM, was investigated. As shown in Fig. 7*A*, the expression levels of integrins β1 and β3 in KSL cells were unaffected after transduction of LentiLox vectors equipped with shRNA sequences for talin-1 and vinculin. Interestingly, adhesion to the ECM in the static condition was significantly inhibited in talin-deficient transduced KSL cells but not in vinculin-deficient transduced KSL cells (Fig. 7*B*). Cell spreading onto fibronectin was also investigated by confocal microscopy. The silencing of talin-1, but not of vinculin, resulted in a failure of cells to spread on fibronectin after adhesion (Fig. 7*C* and supplemental Fig. 5). These results indicate that vinculin is not involved in the attachment and spreading of KSL cells to the ECM in the static condition and that its role in HSC repopulation is independent of integrin function.

DISCUSSION

HSCs are the most thoroughly characterized type of adult stem cells, and the hematopoietic system has served as the principal model for stem cell biology. Transplantation of HSC populations has been shown to be sufficient for long term multilineage reconstitution, not only in experimental animal models but also in clinical patients with hematological malignancies. HSCs must undergo several steps to achieve engraftment after transplantation, including transendothelial migration into the BM (homing), settling in the BM niche (lodging and retention), and intra-BM proliferation and multilineage differentiation (repopulation) (30). The present study showed that HSCs lacking vinculin were unable to reconstitute the hematopoietic sys-

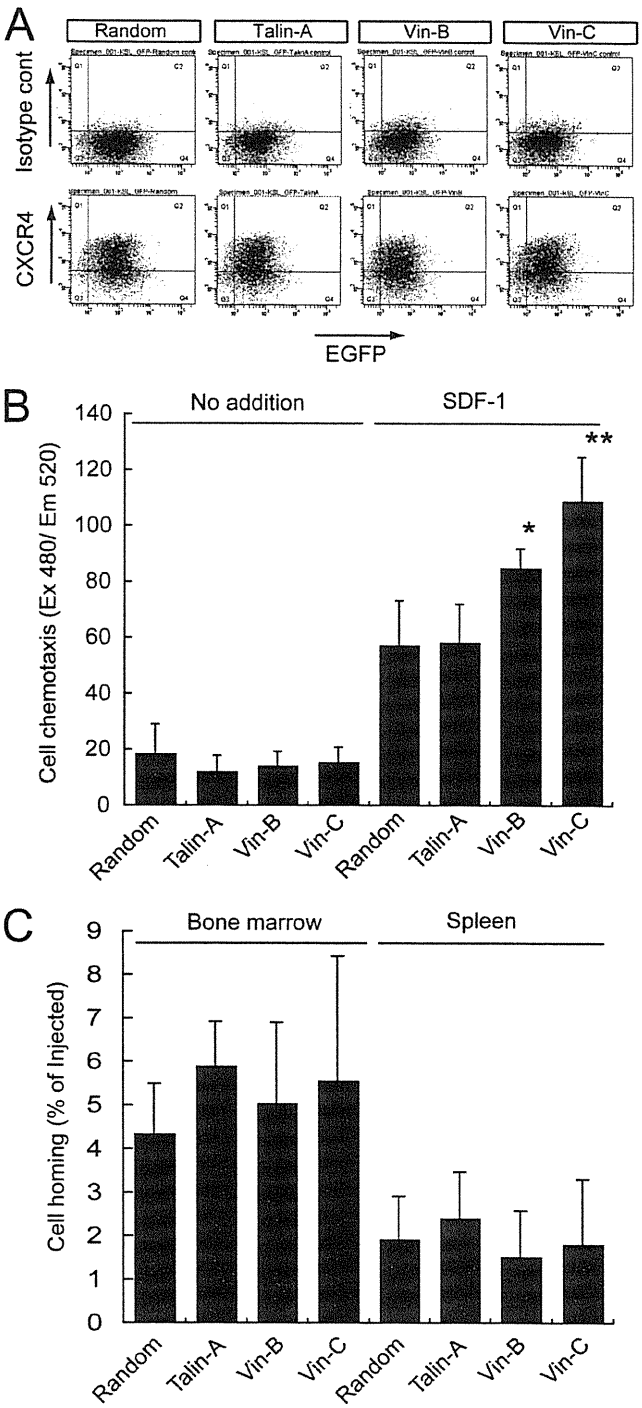

FIGURE 5. **Roles of talin and vinculin in the homing of KSL cells.** *A*, the expression of CXCR4 in KSL cells transduced with the indicated LentiLox vector was evaluated by FACS (*lower panels*). The results for an isotype-matched control Ab are also shown (*upper panels*). *B*, transduced KSL cell migration *in vitro* was assessed using a modified Boyden chamber assay. Stromal cell-derived factor 1 (100 ng/ml) was placed in the lower chamber (or not added), and the cells were allowed to migrate for 4 h. The *columns* and *error bars* represent the means ± S.D. (n = 4). *C*, transduced KSL cells were injected into lethally irradiated recipient mice. The cells from the BM and spleen were collected for CFU-GM assays at 16–20 h after injection. The total numbers of CFU-GM recovered from the BM and spleen were counted manually and expressed as percentages of the number of CFU-GM from the injected KSL cells. The *columns* and *error bars* represent the means ± S.D. (n = 4). *, $p < 0.05$; **, $p < 0.01$, compared with the control experiment (random) under the same conditions (two-tailed Student's t test).

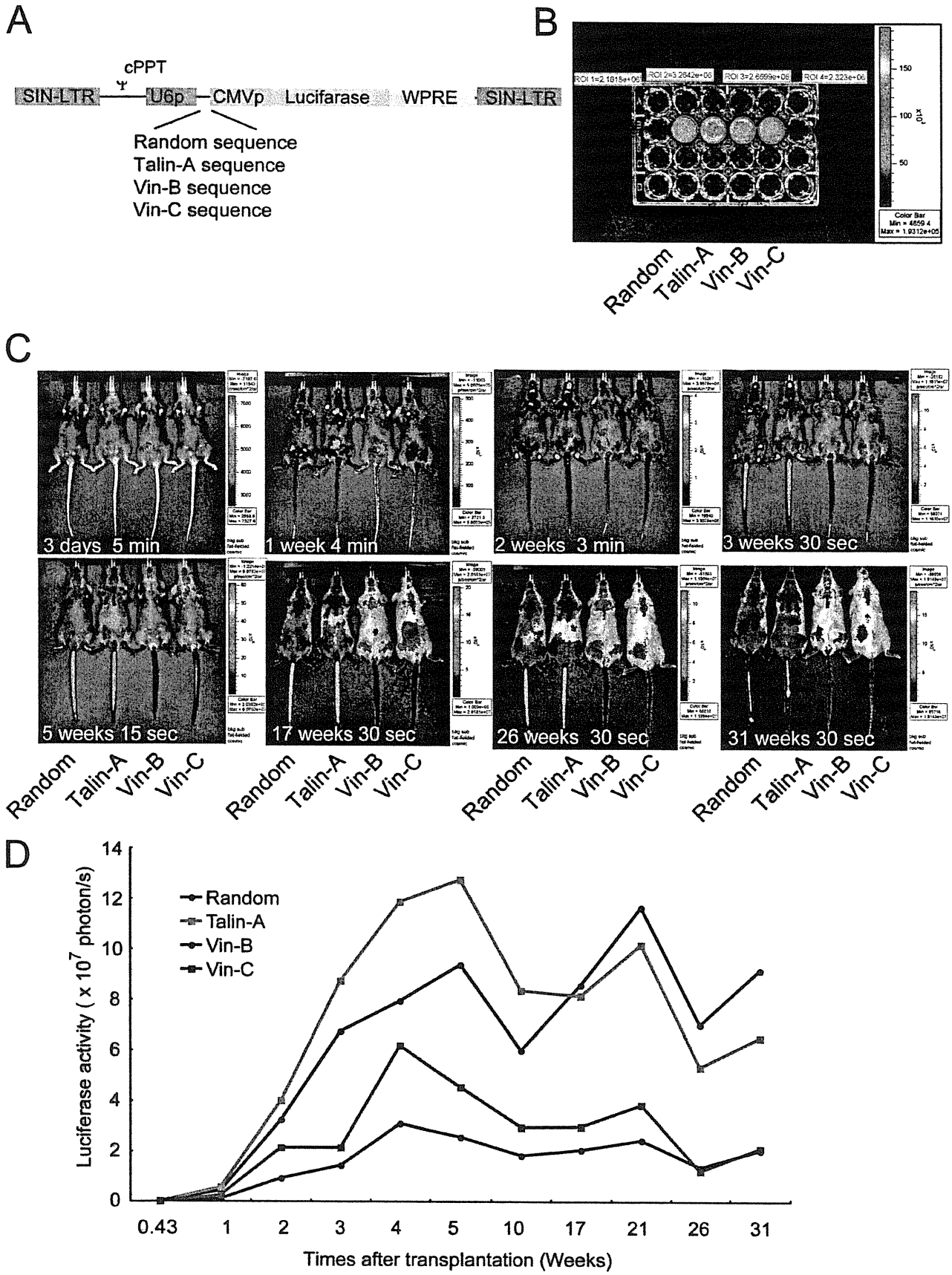

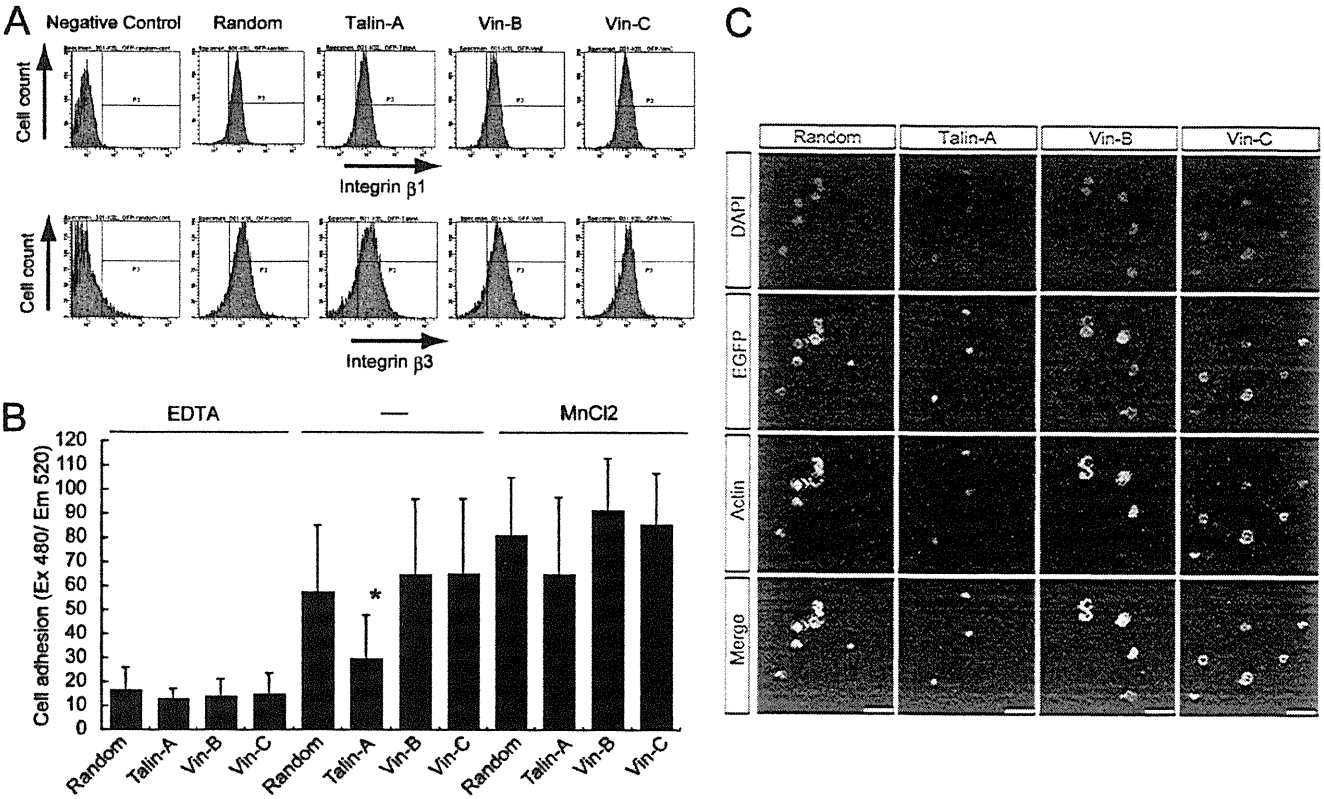

FIGURE 7. **Loss of vinculin does not affect integrin expression and adhesion of KSL cells to the ECM.** KSL cells were transduced with the indicated LentiLox vectors. *A*, the expression levels of integrin β1 (*upper panels*) and integrin β3 (*lower panels*) were examined by FACS. The results for an isotype-matched control Ab are also shown. *B*, cell adhesion to fibronectin (10 μg/ml) in the absence or presence of 2 mM EDTA or 2 mM $MnCl_2$ were assessed as described under "Experimental Procedures." The *columns* and *error bars* represent the means ± S.D. ($n = 4$). *, $p < 0.05$, compared with the control experiment (random) under the same conditions (two-tailed Student's *t* test). *C*, the transduced KSL cells were placed on immobilized fibronectin (10 μg/ml) for 3 h. The cells were fixed and then stained with DAPI (*blue*), anti-GFP antibody (*green*), and rhodamine-conjugated phalloidin (*red*). *Bar*, 40 μm. The data are representative of three independent experiments.

tem efficiently and failed to maintain their self-renewal capacity on BM stromal cell layers. However, the loss of vinculin did not inhibit the potential of HSCs to differentiate into granulocytic and monocytic lineages, *in vitro* migration toward stromal cell-derived factor 1α, and *in vivo* homing to the BM. In addition, HSC adhesion to the ECM was abolished by expression of an shRNA sequence against talin-1, but not vinculin. This suggests that vinculin controls repopulation by HSCs in the BM microenvironment, independent of integrin function.

Cell-cell and cell-ECM interactions have been reported to be crucial for a number of HSC functions in the BM microenvironment (1, 2). Two different niches have been identified in the BM: the endosteal stem cell niche at the endosteum of the bone and the vascular niche in close proximity to the blood vessels. N-cadherin/β-catenin, Tie2/Ang-1, vascular cell adhesion molecule/integrin, and osteopontin/β1 integrin represent important adhesion molecules for the functions of these niches (1, 33). These molecules play roles either in the attachment of HSCs to the niche or in the migration of HSCs. Roles for integrins in HSC homing have been investigated in β1 integrin-knock-out mice and by blocking integrin function with anti-integrin antibodies (6–8). Osteopontin was recently found to contribute to HSC migration toward the endosteal region through its interaction with β1 integrin (34). Interactions between an integrin and the ECM are required for its transition from a low to a high affinity state via signaling referred to as "inside-out signaling" pathways (35). The interaction between an integrin and its ligand triggers signaling that promotes cytoskeletal changes, leading to cell spreading and stabilization through the process termed "outside-in signaling" (36, 37). Proteins that can directly bind to β-integrin cytoplasmic tails are important for these signaling pathways (see the Introduction) (12, 13). Inside-out and outside-in signaling of integrins are often considered separately, but some β integrin cytoplasmic proteins, including talin and cytoplasmic phospholipase A_2, may function in both (38, 39). The reconstitution of HSCs after

FIGURE 6. **Visualization of KSL cell fates *in vivo* in the absence of talin or vinculin.** *A*, schematic presentation of the lentiviral vector used in this experiment. The *EGFP* gene of the LentiLox lentiviral vector was replaced with a *luciferase* gene. *B–D*, KSL cells were transduced with a lentiviral vector expressing a control shRNA sequence (random) or shRNA sequences against talin (Talin-A) or vinculin (Vin-B and Vin-C). *B*, *ex vivo* bioluminescence images of transduced KSL cells before transplantation. *C*, transduced KSL cells together with competitor cells were transplanted into lethally irradiated recipient mice. The photons transmitted through the body were collected for the indicated lengths of time at the indicated days after transplantation using an IVIS Imaging System. *D*, quantitative data for *in vivo* bioluminescence imaging of the mice expressed as photon units (photons/s). The data are representative mean results obtained from two mice after transplantation in two independent experiments.

transplantation was partially impaired under conditions where the adhesion and spreading of HSCs onto ECM (outside-in signaling) were significantly inhibited by silencing of talin-1, whereas homing of HSCs to the BM was not affected. We cannot rule out the possibility that the discrepancy between the current and previous results (6) regarding the role of integrins in HSC homing could be the result of incomplete inhibition of integrin function by silencing of talin-1. However, our results suggest that signaling through integrins expressed in HSCs is involved in reconstitution in the BM microenvironment, although the contribution of talin-1 to integrin activation and HSC reconstitution was much weaker than that of vinculin.

The most important finding of the present study was the ability of vinculin to control HSC repopulation independently of integrin function. Activation of vinculin has been reported to be triggered by talin and actin polymerization, and this activation may strengthen the interactions between integrins and their ligands (40, 41). However, a reduction in the direct interaction between an integrin and its ligand alone cannot readily explain the phenotype of HSCs lacking vinculin, because although the loss of talin expression in HSCs caused severe impairment of integrin function, it only resulted in marginal failure of reconstitution. Vinculin also exists in cadherin-mediated cell-cell contacts and may therefore play an important role in cadherin-mediated cell-cell attachments in the niche, although conflicting results regarding the role of N-cadherin in HSC maintenance have been reported (42, 43). It is also possible that vinculin-deficient HSCs are unable to achieve a balance between self-renewal and differentiation; HSCs maintain the balance between stem cell and differentiated cell populations by choosing between several alternative fates in the BM, such as self-renewal and commitment to differentiation (44, 45). The former ensures preservation of the HSC fate upon cellular division, whereas the latter enables differentiation into multiple lineages (44). In the present study, the expression of shRNA sequences against vinculin significantly abolished the frequency of LTC-IC and the formation of cobblestone-like areas but not the ability of HSCs to differentiate into granulocytic lineage cells, indicating that vinculin may regulate the self-renewal potential of HSCs. A self-renewal division implies that an HSC is permissive in terms of cell cycle entry but restricted from engaging in differentiation, apoptosis, or senescence pathways (44). A number of genes involved in the cell cycle machinery and HOX proteins (INK4A, HoxB4, and HoxA9) have been shown to regulate intrinsic programs in HSCs during the self-renewal process (46). It is possible that vinculin is directly involved in these spatial and temporal control processes responsible for maintaining the intrinsic balance of HSC self-renewal. Indeed, silencing of vinculin induced cell cycle modulation and the induction of apoptosis in KSL HSCs. In a study of vinculin-deficient embryos, vinculin was found to be necessary for normal neural and cardiac development (47). Furthermore, a mouse model involving cardiac myocyte-specific deletion of the vinculin gene resulted in sudden death and dilated cardiomyopathy (48). Although these abnormalities are believed to result from perturbation of integrin-dependent cell functions, the involvement of a specific function of vinculin that is independent of integrins cannot be ruled out, as demonstrated for HSC functions. Further studies are required to address these issues.

Silencing of vinculin failed to inhibit the adhesive properties of HSCs in this study. This was consistent with the results of a recent study indicating that inhibition of vinculin by RNA interference did not affect cell attachment to ECM in epithelial cells (49). Furthermore, silencing of vinculin did not abolish cell spreading of Chinese hamster ovary cells transformed to express integrin αIIbβ3 (αIIbβ3-CHO cells) on fibrinogen (50). This suggests that vinculin may not be involved in the initial attachment to the ECM and outside-in signaling of integrin. However, vinculin might be important for integrin αIIbβ3 inside-out signaling, because the activated form of vinculin (the form inhibiting head-to-tail association) could induce binding of PAC-1 (a monoclonal Ab recognizing activated integrin αIIbβ3) to αIIbβ3-CHO cells (50). Further experiments to investigate the role of vinculin in inside-out signaling of integrins in platelet activation are now underway in our laboratory.

In summary, we have demonstrated that vinculin is required for HSC repopulation after HSC transplantation. These results provide the first evidence for vinculin as an important regulator of cellular functions, independent of integrin function. The manipulation of vinculin expression may represent a novel approach for not only regenerative and developmental medicine but also for the treatment of hematological malignancies. Further studies are needed to determine the precise cellular mechanisms whereby vinculin modulates HSC repopulation independently of integrin function and to apply vinculin-targeting therapies to the treatment of a variety of refractory disorders.

Acknowledgments—We acknowledge Dr. K. Eto (Tokyo University) for helpful discussions. We also thank N. Matsumoto and M. Ito for excellent technical assistance.

REFERENCES

1. Arai, F., and Suda, T. (2007) *Ann. N.Y. Acad. Sci.* **1106,** 41–53
2. Huang, X., Cho, S., and Spangrude, G. J. (2007) *Cell Death Differ.* **14,** 1851–1859
3. Arai, F., Hirao, A., Ohmura, M., Sato, H., Matsuoka, S., Takubo, K., Ito, K., Koh, G. Y., and Suda, T. (2004) *Cell* **118,** 149–161
4. Zhang, J., Niu, C., Ye, L., Huang, H., He, X., Tong, W. G., Ross, J., Haug, J., Johnson, T., Feng, J. Q., Harris, S., Wiedemann, L. M., Mishina, Y., and Li, L. (2003) *Nature* **425,** 836–841
5. Voura, E. B., Billia, F., Iscove, N. N., and Hawley, R. G. (1997) *Exp. Hematol.* **25,** 1172–1179
6. Potocnik, A. J., Brakebusch, C., and Fässler, R. (2000) *Immunity* **12,** 653–663
7. Priestley, G. V., Ulyanova, T., and Papayannopoulou, T. (2007) *Blood* **109,** 109–111
8. Papayannopoulou, T., Craddock, C., Nakamoto, B., Priestley, G. V., and Wolf, N. S. (1995) *Proc. Natl. Acad. Sci. U.S.A.* **92,** 9647–9651
9. van der Loo, J. C., Xiao, X., McMillin, D., Hashino, K., Kato, I., and Williams, D. A. (1998) *J. Clin. Invest.* **102,** 1051–1061
10. Yokota, T., Oritani, K., Mitsui, H., Aoyama, K., Ishikawa, J., Sugahara, H., Matsumura, I., Tsai, S., Tomiyama, Y., Kanakura, Y., and Matsuzawa, Y. (1998) *Blood* **91,** 3263–3272

11. Takada, Y., Ye, X., and Simon, S. (2007) *Genome Biol.* **8,** 215
12. Coller, B. S., and Shattil, S. J. (2008) *Blood* **112,** 3011–3025
13. Zamir, E., and Geiger, B. (2001) *J. Cell Sci.* **114,** 3583–3590
14. Tadokoro, S., Shattil, S. J., Eto, K., Tai, V., Liddington, R. C., de Pereda, J. M., Ginsberg, M. H., and Calderwood, D. A. (2003) *Science* **302,** 103–106
15. Honda, S., Shirotani-Ikejima, H., Tadokoro, S., Maeda, Y., Kinoshita, T., Tomiyama, Y., and Miyata, T. (2009) *Blood* **113,** 5304–5313
16. Ma, Y. Q., Qin, J., Wu, C., and Plow, E. F. (2008) *J. Cell Biol.* **181,** 439–446
17. Moser, M., Nieswandt, B., Ussar, S., Pozgajova, M., and Fässler, R. (2008) *Nat. Med.* **14,** 325–330
18. Tucker, K. L., Sage, T., Stevens, J. M., Jordan, P. A., Jones, S., Barrett, N. E., St-Arnaud, R., Frampton, J., Dedhar, S., and Gibbins, J. M. (2008) *Blood* **112,** 4523–4531
19. Ziegler, W. H., Liddington, R. C., and Critchley, D. R. (2006) *Trends Cell Biol.* **16,** 453–460
20. Izard, T., and Vonrhein, C. (2004) *J. Biol. Chem.* **279,** 27667–27678
21. Papagrigoriou, E., Gingras, A. R., Barsukov, I. L., Bate, N., Fillingham, I. J., Patel, B., Frank, R., Ziegler, W. H., Roberts, G. C., Critchley, D. R., and Emsley, J. (2004) *EMBO J.* **23,** 2942–2951
22. Izard, T., Evans, G., Borgon, R. A., Rush, C. L., Bricogne, G., and Bois, P. R. (2004) *Nature* **427,** 171–175
23. Chen, H., Choudhury, D. M., and Craig, S. W. (2006) *J. Biol. Chem.* **281,** 40389–40398
24. Rubinson, D. A., Dillon, C. P., Kwiatkowski, A. V., Sievers, C., Yang, L., Kopinja, J., Rooney, D. L., Zhang, M., Ihrig, M. M., McManus, M. T., Gertler, F. B., Scott, M. L., and Van Parijs, L. (2003) *Nat. Genet.* **33,** 401–406
25. Ohmori, T., Kashiwakura, Y., Ishiwata, A., Madoiwa, S., Mimuro, J., and Sakata, Y. (2007) *Arterioscler. Thromb. Vasc. Biol.* **27,** 2266–2272
26. Ohmori, T., Mimuro, J., Takano, K., Madoiwa, S., Kashiwakura, Y., Ishiwata, A., Niimura, M., Mitomo, K., Tabata, T., Hasegawa, M., Ozawa, K., and Sakata, Y. (2006) *FASEB J.* **20,** 1522–1524
27. Rawls, A. S., Gregory, A. D., Woloszynek, J. R., Liu, F., and Link, D. C. (2007) *Blood* **110,** 2414–2422
28. Yang, L., Wang, L., Geiger, H., Cancelas, J. A., Mo, J., and Zheng, Y. (2007) *Proc. Natl. Acad. Sci. U.S.A.* **104,** 5091–5096
29. Qian, H., Georges-Labouesse, E., Nyström, A., Domogatskaya, A., Tryggvason, K., Jacobsen, S. E., and Ekblom, M. (2007) *Blood* **110,** 2399–2407
30. Ogaeri, T., Eto, K., Otsu, M., Ema, H., and Nakauchi, H. (2009) *Stem Cells* **27,** 1120–1129
31. Okada, S., Nakauchi, H., Nagayoshi, K., Nishikawa, S., Miura, Y., and Suda, T. (1992) *Blood* **80,** 3044–3050
32. Nakauchi, H., Sudo, K., and Ema, H. (2001) *Ann. N.Y. Acad. Sci.* **938,** 18–25
33. Yin, T., and Li, L. (2006) *J. Clin. Invest.* **116,** 1195–1201
34. Nilsson, S. K., Johnston, H. M., Whitty, G. A., Williams, B., Webb, R. J., Denhardt, D. T., Bertoncello, I., Bendall, L. J., Simmons, P. J., and Haylock, D. N. (2005) *Blood* **106,** 1232–1239
35. Bennett, J. S. (2005) *J. Clin. Invest.* **115,** 3363–3369
36. Takizawa, H., Nishimura, S., Takayama, N., Oda, A., Nishikii, H., Morita, Y., Kakinuma, S., Yamazaki, S., Okamura, S., Tamura, N., Goto, S., Sawaguchi, A., Manabe, I., Takatsu, K., Nakauchi, H., Takaki, S., and Eto, K. *J. Clin. Invest.* **120,** 179–190
37. Phillips, D. R., Nannizzi-Alaimo, L., and Prasad, K. S. (2001) *Thromb. Haemost.* **86,** 246–258
38. Prévost, N., Mitsios, J. V., Kato, H., Burke, J. E., Dennis, E. A., Shimizu, T., and Shattil, S. J. (2009) *Blood* **113,** 447–457
39. Nieswandt, B., Moser, M., Pleines, I., Varga-Szabo, D., Monkley, S., Critchley, D., and Fässler, R. (2007) *J. Exp. Med.* **204,** 3113–3118
40. Schwartz, M. A. (2009) *Science* **323,** 588–589
41. del Rio, A., Perez-Jimenez, R., Liu, R., Roca-Cusachs, P., Fernandez, J. M., and Sheetz, M. P. (2009) *Science* **323,** 638–641
42. Kiel, M. J., Acar, M., Radice, G. L., and Morrison, S. J. (2009) *Cell Stem Cell* **4,** 170–179
43. Kiel, M. J., Radice, G. L., and Morrison, S. J. (2007) *Cell Stem Cell* **1,** 204–217
44. Blank, U., Karlsson, G., and Karlsson, S. (2008) *Blood* **111,** 492–503
45. Martinez-Agosto, J. A., Mikkola, H. K., Hartenstein, V., and Banerjee, U. (2007) *Genes Dev.* **21,** 3044–3060
46. Zon, L. I. (2008) *Nature* **453,** 306–313
47. Xu, W., Baribault, H., and Adamson, E. D. (1998) *Development* **125,** 327–337
48. Zemljic-Harpf, A. E., Miller, J. C., Henderson, S. A., Wright, A. T., Manso, A. M., Elsherif, L., Dalton, N. D., Thor, A. K., Perkins, G. A., McCulloch, A. D., and Ross, R. S. (2007) *Mol. Cell. Biol.* **27,** 7522–7537
49. Peng, X., Cuff, L. E., Lawton, C. D., and DeMali, K. A. (2010) *J. Cell Sci.* **123,** 567–577
50. Ohmori, T., Kashiwakura, Y., Ishiwata, A., Madoiwa, S., Mimuro, J., Honda, S., Miyata, T., and Sakata, Y. (2010) *Biochem. Biophys. Res. Commun.*, in press